NEUTAG: Graph Transformer for Attributed Graphs

Shubham Gupta *shubham.gupta@cse.iitd.ac.in*
Department of Computer Science and Engineering
Indian Institute of Technology Delhi, New Delhi

Sayan Ranu *sayanranu@cse.iitd.ac.in*
Department of Computer Science and Engineering
Indian Institute of Technology Delhi, New Delhi

Srikanta Bedathur *srikanta@cse.iitd.ac.in*
Department of Computer Science and Engineering
Indian Institute of Technology Delhi, New Delhi

Reviewed on OpenReview: *https://openreview.net/forum?id=kQrIrYvbbw*

Abstract

Graph Transformers (GT) have demonstrated their superiority in graph classification tasks, but their performance in node classification settings remains below par. They are designed for either homophilic or heterophilic graphs and show poor scalability to million-sized graphs. In this paper, we address these limitations for node classification tasks by designing a model that utilizes a special feature encoding that transforms the input graph separating nodes and features, which enables the flow of information not only from the local neighborhood of a node but also from distant nodes, via their connections through shared feature nodes. We theoretically demonstrate that this design allows each node to exchange information with all nodes in the graph, effectively mimicking all-node-pair message passing without requiring dense attention between all node pairs. This enables scalability for large attributed graphs when the number of features is substantially smaller than the number of nodes. We further analyze the universal approximation ability of the proposed transformer. Finally, we demonstrate the effectiveness of the proposed method on diverse sets of large-scale graphs, including the homophilic & the heterophilic varieties.

1 Introduction

Graph neural networks (GNN) (Hamilton et al., 2017; Veličković et al., 2018; Xu et al., 2019; Abu-El-Haija et al., 2019; Nishad et al., 2021) are increasingly considered de facto models for solving graph mining tasks such as graph classification, node classification, link prediction, etc. Their utility has been demonstrated across diverse domains, including drug and material discovery Goyal et al. (2020); Bihani et al. (2023), traffic forecasting Gupta et al. (2023); Jain et al. (2021), recommendation systems Gupta et al. (2025); Sirohi et al. (2024), and modeling physical interacting systems Bishnoi et al. (2024; 2023); Bhattoo et al. (2022). Recent advances in the transformer (Vaswani et al., 2017) family of neural networks, especially in the domain of language (Devlin et al., 2019; Radford et al., 2019), and vision (Dosovitskiy et al., 2020) have propelled their applications in the graph domain as well, specifically for graph classification tasks (Rampášek et al., 2022). Graph Transformers (GT) take node sequences as input with their attributes, structural and position encoding, and apply transformer layers (Vaswani et al., 2017) successively to learn contextual node representation. It enables modeling long-range dependencies among nodes, avoids over-smoothing (Liu et al., 2020) problems linked with deeper GNN, and is more expressive due to structural (Dwivedi et al., 2022a) and position encodings (Kreuzer et al., 2021a; Dwivedi et al., 2023a). These advantages in the GT architecture

lead them to outperform other GNN-based methods, especially in molecular and biological graph classification tasks, as shown in GRAPHGPS (Rampášek et al., 2022).

However, the sizes of graphs considered in graph classification tasks are typically of small scale, that is, $\approx$ 100 nodes per graph. In contrast, node classification tasks often involve graphs with millions of nodes, such as snap-patents (Lim et al., 2021). One of the fundamental limitations of using graph transformers in these settings is dense attention, which computes attention over all node pairs, leading to $\mathcal{O}(N^2)$ computation per layer. This is computationally prohibitive and not practical for applications involving large graphs. Recently, sparse-attention methods (Choromanski et al., 2020; Zaheer et al., 2021) proposed in language models have been utilized in GT (Rampášek et al., 2022) to approximate dense attention. However, these sparse-attention methods don't explicitly leverage the structural properties of graphs, resulting in sub-optimal performance than dense attention-based graph transformers. Recently, graph-specific sparse transformers (Rampášek et al., 2022; Shirzad et al., 2023; Kong et al., 2023; Chen et al., 2022b) have been proposed to incorporate graph topology, which learn virtual tokens via global nodes, anchor nodes, or clustering. However, none of these methods explicitly uses the feature dimension as a carrier for long-range communication.

1.1 Existing Works and their limitations

A plethora of graph transformers have been proposed to target many aspects of representation learning. A recent survey (Müller et al., 2024) characterizes these key innovations into four primary dimensions: 1) the design of positional and structural encodings (Chen et al., 2022a; Dwivedi et al., 2022a; Bouritsas et al., 2021; Kreuzer et al., 2021b; Lim et al., 2023; Dwivedi & Bresson, 2021; Wang et al., 2022), 2) handling of geometric vs non-geometric features (Fuchs et al., 2020; 2021; Shi et al., 2023; Luo et al., 2023), 3) graph tokenization (Kim et al., 2022; Hussain et al., 2022; Chen et al., 2022b), and 4) propagation mechanisms (Rampášek et al., 2022; Shirzad et al., 2023; Kong et al., 2023; Chen et al., 2022b; Dwivedi et al., 2023b; Ma et al., 2023; Liu et al., 2023; Kuang et al., 2021; Zhu et al., 2024; Liu et al., 2023). We have additionally identified a fifth dimension focusing on replacing standard self-attention formulae with equivalent, scalable formulations using linear, polynomial and diffusion processes based kernels (Wu et al., 2023a;b; Deng et al., 2024). These improve scalability but at the cost of expressivity (Deng et al., 2024) and still require graph partitioning on million-sized graphs, breaking all-pair connectivity.

This paper focuses primarily on the fourth category, which aims to approximate all pair attention connectivity. These methods typically adopt a common modular architecture. Each layer is composed of a message-passing neural network (MPNN) (Hamilton et al., 2017; Veličković et al., 2018; Xu et al., 2019) followed by a transformer layer. The principal distinctions between methods lie in the design of the transformer layer. GRAPHGPS utilizes all-pairs attention. EXPHORMER combines GNN with a transformer layer consisting of local neighbor attention and non-local attention via virtual nodes. These virtual nodes are connected to every node in the graph, leading to an approximation of all-node-pairs attention.GOAT (Kong et al., 2023) and LARGEGT (Dwivedi et al., 2023b) removes the GNN component entirely by replacing virtual nodes in EXPHORMER using trainable and clustering-based virtual nodes maintained using a code-book computed by k-means clustering and updated through exponentially moving averages.

- **Redundant dependency on Gnn:** Hybrid GT such as GRAPHGPS and EXPHORMER utilize a modular architecture of GNN and transformers. While effective, this creates redundant dependence, despite the literature showing that Transformers with positional/structural encodings are theoretically universal approximators of graph-to-graph functions (Yun et al., 2020; Kreuzer et al., 2021a).
- **Limited to either homophilic or heterophilic graphs:** Hybrid architectures inherit the biases of the underlying GNN. If GNN derives the node representation mainly from its local connectivity, then it will propagate homophily biases in the transformer. Similarly, if a GNN is designed for heterophilic graphs that use higher-hop nodes, it will propagate non-homophily biases in the transformer. For example, EXPHORMER and GRAPHGPS use GCN (Kipf & Welling, 2017) as GNN, which leads to their good performance on homophilic graphs (Sen et al., 2008; Yang et al., 2016) but not on heterophilic graphs (Pei et al., 2020; Rozemberczki et al., 2021; Lim et al., 2021). We show this effect empirically in Table 1, where we remove the GCN component to show how their performance improves on heterophilic graphs but reduces on homophilic graphs.

- **Non-scalable or assumptions based:** Dense-attention and global token-based transformers (Rampášek et al., 2022; Shirzad et al., 2023) require the full graph in GPU memory, making training on large graphs challenging. Linear-attention variants (Wu et al., 2023a; Deng et al., 2024; Wu et al., 2023b) improve memory efficiency and increase scalability, but still require graph partitioning for million-node datasets, which breaks all-pairs attention and often sacrifices expressivity due to kernel approximations (Deng et al., 2024). Clustering-based virtual node methods (Kong et al., 2023; Dwivedi et al., 2023b; Zhu et al., 2024) avoid GNN reliance but require a trainable projection matrix and tuning of the number of virtual nodes.

1.2 Contributions

To address the gaps outlined above, we propose Neural Transformer for Attributed Graphs (NEUTAG). We use graph transformations with node features as virtual nodes to design novel sparse graph transformers. We examine the benefits of the aforementioned transformation, including increased graph homophily. In summary, NEUTAG offers the following significant advantages over the existing work.

- **Scalable and data-agnostic modeling for attributed graphs:** NEUTAG transforms the input graph into a bipartite structure consisting of graph nodes and virtual feature nodes, and sparsifies the all-pair attention into a unified attention mechanism over local neighbors and virtual feature neighbors. This allows NEUTAG to flexibly learn from both homophilic patterns via local structures and heterophilic patterns via non-local feature nodes, leading to a data-agnostic architecture. And, since its virtual nodes are based on features that are derived deterministically from the input attribute space rather than learned through a clustering mechanism, NEUTAG avoids the need for clustering-based virtual-node construction. The resulting sparse-attention mechanism seamlessly facilitates node batching and enables NEUTAG to scale to large attributed graphs when the average number of connected features per node is substantially smaller than the graph size.
- **Theoretical analysis:** We establish the theoretical grounding of the proposed transformation by proving that it increases the connectivity in the graph. Moreover, we investigate the theoretical and parameter conditions under which the NEUTAG potentially serves as a permutation-equivariant universal approximator of a dense attention layer.
- **Empirical evaluation:** We perform extensive experiments on real-world datasets, including both homophilic and heterophilic datasets, along with a large-scale dataset *snap-patent* containing 2.9 million nodes and 13.9 million edges. We evaluate our proposed method against 12 graph transformer baselines, including 15 variants. We clearly establish that the proposed sparse graph transformer NEUTAG is competitive in both homophilic and heterophilic graphs, as well as in small-scale and large-scale graphs, consistently.

Paper organization: Section A in appendix introduces preliminaries on graphs, graph neural networks, transformers, and graph transformers, along with notations and problem formulation. Section 3 presents our proposed methodology: we first describe the graph transformation and its benefits for structural connectivity, then introduce the attention mechanism on the transformed graph and analyze its all-pair attention approximation capabilities. Section 4 details the experimental setup, including datasets, baselines, evaluation metrics, and benchmarks NEUTAG. Finally, Section 6 concludes the paper.

2 Preliminaries

We provide preliminaries on Graphs, Graph Neural Networks, Transformers, and Graph Transformers, including definitions, notations, and problem formulation in Appendix A.

3 Methodology

This section presents two main components. First, we propose a graph transformation that decouples features from nodes into separate nodes, improving structural connectivity and increasing effective homophily, which we formally analyze. Building on this transformation, we introduce a novel attention mechanism that facilitates information flow between graph and feature nodes.

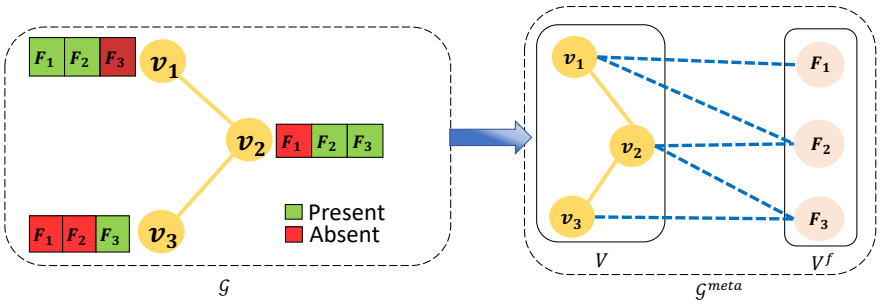

Figure 1: Transformation of input graph $\mathcal{G}$ into its metamorphosis form $\mathcal{G}^{meta}$. In $\mathcal{G}$, the features marked in green are present for the corresponding node. $\mathcal{G}^{meta}$ contains additional edges with all present features.

3.1 Graph transformation

Given a graph $\mathcal{G} = (\mathcal{V}, \mathcal{E}, \mathbf{X})$ and its feature set $\mathcal{F}$ as defined in def. 1 in appendix A where $\mathcal{F} = \bigcup_{v \in \mathcal{V}} \mathcal{F}_v$ is the set of all features in graph $\mathcal{G}$. $\mathcal{F}_v$ is a feature set at node $v \in \mathcal{V}$ we convert it to its metamorphosis form $\mathcal{G}^{meta} = (\mathcal{V}^{meta}, \mathcal{E}^{meta}, \mathbf{X})$ as follows. First, we create virtual feature nodes V^f corresponding to feature set $\mathcal{F}$ of graph $\mathcal{G}$ and add these new nodes to $\mathcal{V}$ to create $\mathcal{V}^{meta}$. Formally,

$$\mathcal{V}^{meta} = \mathcal{V} \cup \mathcal{V}^f : \mathcal{V}^f = \{f \in \mathcal{F}\} \tag{1}$$

Next, we retain the original edges $\mathcal{E}$ in $\mathcal{G}^{meta}$ and create the edges that connect original graph nodes $\mathcal{V}^G$ and $\mathcal{V}^f$ as follows.

$$\mathcal{E}^f = \{(v, f) \mid v \in \mathcal{V}, f \in \mathcal{F}, \mathbf{X}[v, f] = 1\} \tag{2}$$

We overload the matrix index operation with the access operator []. $\mathcal{E}^f$ represents the set of edges between graph nodes $\mathcal{V}$ and features which are present in corresponding nodes. Thus, edges in $\mathcal{G}^{meta}$ consist of original edges and feature edges. Formally,

$$\mathcal{E}^{meta} = \mathcal{E} \cup \mathcal{E}^f \tag{3}$$

Figure 1 illustrates this transformation.Since every node in $\mathcal{G}^{meta}$ has two types of neighbors, we specify each possible neighborhood.

1) Graph neighborhood: nodes from the original graph, $\{\mathcal{N}_v^{\mathcal{G}} = (u \mid (u, v) \in \mathcal{E}\}$,

2) Feature neighborhood for graph nodes: feature nodes $\{\mathcal{N}_v^f = (u \mid (u, v) \in \mathcal{E}^f\}\ \ \forall v \in \mathcal{V}$

3) Graph neighborhood for features nodes: graph nodes $\{\mathcal{N}_f^{\mathcal{G}} = (u \mid (u, f) \in \mathcal{E}^f\}\ \ \forall f \in \mathcal{V}^f$.

3.2 Transformation Benefits

In dense attention, each node ingests information from every other node in a single hop, which requires $\mathcal{O}(N^2)$ computations. The proposed transformation enables nodes to exchange information with *non-local* nodes indirectly via feature nodes, thereby avoiding the explicit computation of pairwise attention scores. This transformation preserves the locality biases and induces connections to distant nodes using feature-connectivity biases. Thus, such transformations increase modeling capacity by incorporating long-range interactions to learn inductive biases of both homophilic and heterophilic graphs.

Connectivity analysis: We assume $D^{\mathcal{G}}$ to be the average graph node degree of graph nodes $\mathcal{V}$, D^F to be the average no. of features for graph nodes $\mathcal{V}$, and $F^{\mathcal{G}}$ be average no. of nodes per feature nodes $\mathcal{V}^f$. We now show that the transformation drastically increases the connectivity in the following theorem.

Theorem 1 (Approximate Connectivity in $\mathcal{G}^{meta}$). *Assuming a tree-like neighborhood expansion and ignoring repeated nodes, the average connectivity of a node in an L-hop neighborhood in an input graph $\mathcal{G}$ grows as $\mathcal{O}((D^{\mathcal{G}})^L)$. Let $\mathcal{G}^{meta}$ be a proposed transformed variant of $\mathcal{G}$. The L-hop neighborhood of same graph node in $\mathcal{G}^{meta}$ grows approximately as $\mathcal{O}((D^{\mathcal{G}})^L + (D^F)^{L/2} * (F^{\mathcal{G}})^{L/2})$.*

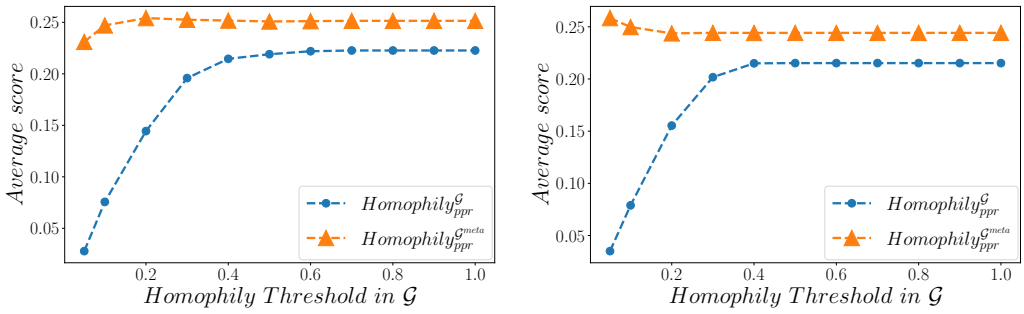

(a) Chameleon (b) Actor

Figure 2: Increase in homophily observed in the transformed graph $\mathcal{G}^{meta}$, while the homophily was low in the original graph $\mathcal{G}$. K is chosen as 50.

Proof: See App. B.1. □.

Generally $D^F > D^{\mathcal{G}}$ and $F^{\mathcal{G}} \gg D^{\mathcal{G}}$ in real world graphs. This leads to a significant increase in connectivity. The enhanced connectivity leads to quicker reachability to long-range nodes, facilitating distant nodes to become higher personalized rank nodes(Page et al., 1999) for target nodes.

Corollary 1. $\mathcal{G}^{meta}$ facilitates long-distance nodes in $\mathcal{G}$ to have better personalized page ranks (PPR) from a target node by introducing additional short paths through feature nodes.

Proof: See App. B.2.

Higher homophily: The increased connectivity due to the proposed transformation leads to higher homophily in top PPR nodes in heterophilic graphs. We demonstrate this empirically on two heterophilic graphs, Actor and Chameleon. We compute the top-K nearest PPR nodes for all graph nodes in $\mathcal{G}$ and $\mathcal{G}^{meta}$ and compute the following homophily score per node. $\forall v \in \mathcal{V}$,

$$Homophily^{\mathcal{G}}_{ppr}(v) = \sum_{i=1}^{i=K} \frac{\mid y(v) = y(ppr^{\mathcal{G}}_i(v)) \mid}{K} \tag{4}$$

where $y(v)$ denotes the label of node v, $ppr_i(v)^{\mathcal{G}}$ denotes the i^{th} nearest PPR nodes from node v when computed on graph $\mathcal{G}$. We compute the scores for graph nodes on graph $\mathcal{G}$ and $\mathcal{G}^{meta}$. We find that $Homophily_{ppr}$ increases in $\mathcal{G}^{meta}$ for nodes who had lower $Homophily_{ppr}$ in the original graph. To demonstrate this, we define a homophily threshold to identify nodes whose score is less than the threshold in $\mathcal{G}$. Finally, we compare their average homophily score in $\mathcal{G}$ with the same identified nodes in $\mathcal{G}^{meta}$. Their homophily score increases drastically in G^{meta}. We note that during top-K ppr node computation in $\mathcal{G}^{meta}$, we pick only graph nodes, disregarding feature nodes $\mathcal{V}^f$. Figure 2 establishes this phenomenon. The difference reduces once the threshold increases more than 0.5.

Next, we discuss our novel attention mechanism on the transformed graph $\mathcal{G}^{meta}$.

3.3 Graph Transformer

The main contribution of this work is to propose features that transform an N dimensional node subspace into a lower F-dimensional feature subspace, enabling attention computation over feature nodes rather than graph nodes where $F = |\mathcal{F}|$. Specifically, we can construct a node-feature incidence matrix, $\mathbf{M} \in \{0,1\}^{N \times F}$ where $\mathbf{M}[i][j] = 1$ when feature j is available in i^{th} node. This projection matrix can reduce the complexity of the core attention operation $\text{SOFTMAX}(\mathbf{X}\mathbf{W}_Q(\mathbf{X}\mathbf{W}_K)^T/\sqrt{d})\mathbf{X}\mathbf{W}_V$ with $\text{SOFTMAX}((\mathbf{X}\mathbf{W}_Q(\mathbf{X}\mathbf{W}_K)^T/\sqrt{d})\mathbf{M})\mathbf{M}^T\mathbf{X}\mathbf{W}_V$ where $\mathbf{W}_Q, \mathbf{W}_K, \mathbf{W}_V \in \mathbb{R}^{d \times d}$. This projection matrix $\mathbf{M}$ facilitates to project $\mathbf{X}\mathbf{W}_K, \mathbf{X}\mathbf{W}_V \in \mathbb{R}^{N \times d}$ to $\mathbb{R}^{F \times d}$ by multiplying by $\mathbf{M}$, thus reducing the computation to $\mathbb{O}(N * F * d)$ much less than $\mathbb{O}(N * N * d)$ when $F \ll N$. Moreover, unlike virtual token-based methods, which

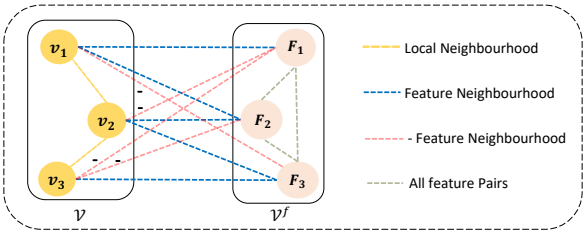

Figure 3: Various attention paths in NEUTAG.

learn the projection matrix $\mathbf{M}$ during training, this approach proposes a fixed, easily derivable projection matrix $\mathbf{M}$. We later discuss the approximation capabilities of this approach in Theorem 2.

NEUTAG architecture constructs the attention graph consisting of 4 types of undirected attention edges as shown in fig 3. These attention paths are applied successively across each layer of NEUTAG. The input to the NEUTAG is the node features $\mathbf{X}$, graph topology $\mathcal{E}$, and position encodings (PE) based on random-walk/Laplacian eigenvalue. The input feature matrix is initialized as

$$\mathbf{H}^0_{\mathcal{V}} = (\mathbf{X} + \mathbf{PE})\mathbf{W} \tag{5}$$

where $\mathbf{H}^0_{\mathcal{V}} \in \mathbb{R}^{N\times d}$ is a initial representation of graph nodes $\mathcal{V}$. Similarly, for feature nodes $\mathcal{V}^f$, we initialize their embedding to randomly initialized random vectors.

$$\mathbf{H}^0_{\mathcal{V}^f}[f] = w_f \in \mathcal{R}^d \;\; \forall f \in \mathcal{V}^f \tag{6}$$

Now, given $\mathbf{H}^{l-1}_{\mathcal{V}} \in \mathbb{R}^{N\times d}$, and $\mathbf{H}^{l-1}_{\mathcal{V}^f} \in \mathbb{R}^{F\times d}$, we first compute the following query, key, and value matrices for both graph nodes and feature nodes respectively.

$$\mathbf{Q}^l_{\mathcal{V}} = \mathbf{H}^{l-1}_{\mathcal{V}}\mathbf{W}^l_1,\; \mathbf{K}^l_{\mathcal{V}} = \mathbf{H}^{l-1}_{\mathcal{V}}\mathbf{W}^l_2,\; \mathbf{V}^l_{\mathcal{V}} = \mathbf{H}^{l-1}_{\mathcal{V}}\mathbf{W}^l_3 \tag{7}$$

$$\mathbf{Q}^l_{\mathcal{V}^f} = \mathbf{H}^{l-1}_{\mathcal{V}^f}\mathbf{W}^l_4,\; \mathbf{K}^l_{\mathcal{V}^f} = \mathbf{H}^{l-1}_{\mathcal{V}^f}\mathbf{W}^l_5,\; \mathbf{V}^l_{\mathcal{V}^f} = \mathbf{H}^{l-1}_{\mathcal{V}^f}\mathbf{W}^l_6 \tag{8}$$

Now we define the following attentions to compute $\mathbf{H}^l_{\mathcal{V}}$ and $\mathbf{H}^l_{\mathcal{V}^f}$. Please note that we provide details using one head for simplicity, but we employ multi-head attention as prevalent in transformers, which entails running attention H times and concatenating these outputs.

Local neighborhood attention: Local neighborhood plays a critical role in node classification accuracy and is commonly used in every sparse transformer, e.g. GRAPHGPS, EXPHORMER, GOAT, LARGEGT, and NAGPHORMER. For each target graph node $v \in \mathcal{V}$, the following vector is computed.

$$\mathbf{H}^l_{\mathcal{V}:local}[v] = \sum_{u\in\mathcal{N}^{\mathcal{G}}_v} \frac{\exp(\mathbf{Q}^l_{\mathcal{V}}[v] * \mathbf{K}^l_{\mathcal{V}}[u]/\sqrt{d})}{\sum_{u'\in\mathcal{N}^{\mathcal{G}}_v}\exp(\mathbf{Q}^l_{\mathcal{V}}[v] * \mathbf{K}^l_{\mathcal{V}}[u']/\sqrt{d})}\mathbf{V}^l_{\mathcal{V}}[u] \tag{9}$$

We apply all-pair attention for each feature node $f \in \mathcal{V}^f$ to compute their local representation at layer l.

$$\mathbf{H}^l_{\mathcal{V}^f:local} = \text{SOFTMAX}\left(\frac{\mathbf{Q}^l_{\mathcal{V}^f}(\mathbf{K}^l_{\mathcal{V}^f})^T}{\sqrt{d}}\right)\mathbf{V}^l_{\mathcal{V}^f} \tag{10}$$

Attention using feature connections: The next component utilizes graph nodes to feature nodes connections and vice-versa to learn non-local representations.

For graph nodes $\forall v \in \mathcal{V}$, we use the following.

$$\mathbf{H}^l_{\mathcal{V}:+}[v] = \sum_{f\in\mathcal{N}^f_v} \frac{\exp(\mathbf{Q}^l_{\mathcal{V}}[v] * \mathbf{K}^l_{\mathcal{V}^f}[f]/\sqrt{d})}{\sum_{f'\in\mathcal{N}^f_v}\exp(\mathbf{Q}^l_{\mathcal{V}}[v] * \mathbf{K}^l_{\mathcal{V}^f}[f']/\sqrt{d})}\mathbf{V}^l_{\mathcal{V}^f}[f] \tag{11}$$

For feature nodes $\forall f \in \mathcal{V}^f$, we compute the following.

$$\mathbf{H}^l_{\mathcal{V}^f:+}[f] = \sum_{u \in \mathcal{N}^{\mathcal{G}}_f} \frac{\exp(\mathbf{Q}^l_{\mathcal{V}^f}[f] * \mathbf{K}^l_{\mathcal{V}}[u]/\sqrt{d})}{\sum_{u' \in \mathcal{N}^{\mathcal{G}}_f} \exp(\mathbf{Q}^l_{\mathcal{V}^f}[f] * \mathbf{K}^l_{\mathcal{V}}[u']/\sqrt{d})} \mathbf{V}^l_{\mathcal{V}}[u] \tag{12}$$

Attention using absent feature connections Since absent features also provide valuable *exclusion* information for node classification, we define negative feature edges as follows.

$$\mathcal{E}^{f-} = \{(v, f) \mid v \in \mathcal{V}, f \in F, \mathbf{X}[v, f] = 0\} \tag{13}$$

Corresponding to negative edges, we define the negative feature neighborhood for graph nodes $V^{\mathcal{G}}$ as $\{\mathcal{N}^-_v = (u \mid (u, v) \in \mathcal{E}^{f-}\}$.

Similar to eq. 9 and 11, we utilize the negative graph connections between graph nodes, and feature node connections are utilized as follows. $\forall v \in \mathcal{V}$,

$$\mathbf{H}^l_{\mathcal{V}:-}[v] = \sum_{f \in \mathcal{N}^-_v} \frac{\exp(\mathbf{Q}^l_{\mathcal{V}}[v] * \mathbf{K}^l_{\mathcal{V}^f}[f]/\sqrt{d})}{\sum_{f' \in \mathcal{N}^-_v} \exp(\mathbf{Q}^l_{\mathcal{V}}[v] * \mathbf{K}^l_{\mathcal{V}^f}[f']/\sqrt{d})} \mathbf{V}^l_{\mathcal{V}^f}[f] \tag{14}$$

Since each graph node has multiple negative features, we sample a fixed number of negative-feature nodes per node using degree-based sampling to improve implementation efficiency.

Finally, these local and non-local representations are merged to learn next-layer representations of graph and feature nodes as follows.

$$\mathbf{H}^l_{\mathcal{V}} = \textsc{update}^l_1(\mathbf{H}^{l-1}_{\mathcal{V}}, \textsc{mlp}^l_1(\mathbf{H}^l_{\mathcal{V}:local} \mid \mathbf{H}^l_{\mathcal{V}:+} \mid \mathbf{H}^l_{\mathcal{V}:-})) \tag{15}$$

$$\mathbf{H}^l_{\mathcal{V}^f} = \textsc{update}^l_2(\mathbf{H}^{l-1}_{\mathcal{V}^f}, \textsc{mlp}^l_2(\mathbf{H}^l_{\mathcal{V}^f:local} \mid \mathbf{H}^l_{\mathcal{V}^f:+})) \tag{16}$$

Here $\textsc{update}^l$ can be a neural net-based functions, e.g. MLP or skip-connections.

Computational Complexity: Considering all attention components, per-layer complexity of NEUTAG is $\mathcal{O}(Nd^2 + Fd^2 + |\mathcal{E}|d + |\mathcal{E}^f|d + F^2d + Nrd)$ where the first and second terms correspond to linear projections of graph nodes and feature nodes, respectively. The term $|\mathcal{E}|d$ corresponds to the cost of local neighborhood attention, and $|\mathcal{E}^f|d$ corresponds to node-to-feature and feature-to-node attention scaling with node-feature edges. The term F^2d corresponds to feature-feature attention and Nrd to sampled negative feature attention, where r is the number of negative features per node and is small. We note that this complexity is upper-bounded by $\mathcal{O}(NFd)$ in the extreme case where all graph nodes are connected with all feature nodes. In practice, for a large-scale graph where $F \ll N$ yields $\mathcal{O}(NFd) \ll \mathcal{O}(N^2d)$, enabling scalability of NEUTAG to large-scale datasets. For small-scale datasets where $F = \mathcal{O}(N)$, the computational advantage diminishes over dense attention-based graph transformers. However, proposed novel attention paths through feature nodes still enable effective modeling of both homophilic and heterophilic graphs.

We now show that NEUTAG approximates the Positive Orthogonal Random Projections based sparse-transformer PERFORMER (Choromanski et al., 2020), which kernelizes the softmax operation using Mercer's theorem. We formally define the following theorem.

Theorem 2. *Under the stated assumptions, NEUTAG can approximate the following PERFORMER self-attention layer applied to the l^{th} layer node representation $\mathbf{H}^l$ of graph $\mathcal{G}$, using at most* **4** *attention layers:*

$$\mathbf{h}^{l+1}_i = \frac{\phi(\mathbf{W}_Q \mathbf{h}^l_i)^T \sum_{j=1}^{j=N} \phi(\mathbf{W}_K \mathbf{h}^l_j) \otimes (\mathbf{W}_V \mathbf{h}^l_j)}{\phi(\mathbf{W}_Q \mathbf{h}^l_i) \sum_{k=1}^{k=N} \phi(\mathbf{W}_K \mathbf{h}^l_k)} \tag{17}$$

This holds under the following assumptions: (a) the kernel feature map ϕ can be approximated by neural networks, and (b) each graph node is connected to at least one feature node. Here, $\mathbf{h}_i = \mathbf{H}[i] \in \mathbb{R}^d$, $\mathbf{W}_Q, \mathbf{W}_K, \mathbf{W}_V$ are learnable weight matrices, and $\phi : \mathbb{R}^d \to \mathbb{R}^m$ is a low-dimensional feature mapping.

Proof: See App. B.3. □.

Moreover, "at most 4 layer" result in theorem 2 is a theoretical expressivity result, showing NEUTAG can approximate a PERFORMER-style attention. The result establishes that such an approximation is *possible* within 4 layer, but it doesn't imply that fewer layers can't learn an effective representation. Moreover, it also doesn't imply that exactly 4 layers are required in empirical settings, which might depend on dataset characteristics and the nature of the downstream task. Moreover, we analyze NEUTAG's theoretical capabilities to approximate dense-attention in Appendix B.4.

Extension of Neutag to continuous-valued attributed graphs: Section C also discusses the extension of NEUTAG on continuous-attributed datasets.

3.4 Neutag Mini-Batching

The proposed framework is applicable for **a) Small graphs** by running forward pass on entire graph $\mathcal{G}^{meta}$ and **b) Large-scale graphs** by offline sampling L layer directed sub-graphs from feature nodes $\mathcal{V}^f$ to graph nodes $\mathcal{V}$ from $\mathcal{G}^{meta}$, as these sub-graphs will be common among all batches of graph nodes $\mathcal{V}$ and run NEUTAG on such constructed batches and back-propagate. Algorithm 1 summarizes the creation of a mini-batch for a large-scale graph for NEUTAG training and inference. Specifically, for each feature node $v^f \in \mathcal{V}^f$, graph nodes are sampled in line 4. Corresponding to these graph nodes, the L hop sub-graph is sampled in the original node space $\mathcal{V}$. Please note that data from lines 3-12 can be cached across multiple batches and performed offline. Finally, a batch of nodes is sampled from the input graph, and the corresponding L-HOP subgraph is sampled. Finally, feature edges are added to correspond to these sampled original graph nodes.

4 Experiments

4.1 Empirical Evaluation

We now evaluate the effectiveness of NEUTAG on node classification tasks across diverse graph datasets and examine its robustness with state-of-the-art graph transformers(GT). We also compare NEUTAG with standard Graph Neural Networks (GNN). Finally, we analyze the importance of feature nodes based on the attention layer via an ablation study. We also analyze the impact of feature sparsity or missing features on NEUTAG's performance in the appendix section E.3.

4.2 Datasets

Table 5 in appendix D.1 summarizes the datasets and their statistics. Cora (Sen et al., 2008), CiteSeer (Yang et al., 2016) and OGBN-Arxiv (Hu et al., 2020) are homophilic datasets while Actor (Pei et al., 2020), Chameleon (Rozemberczki et al., 2021), OGBN-Arxiv(year) (Hu et al., 2020) and Snap-Patents (Lim et al., 2021) are heterophilic datasets. Out of these, Snap-Patents is the largest dataset, having 2.92 million nodes and 13.97 million edges. We use 60%, 20%, and 20% train, validation, and test splits on all datasets for all methods, including baselines. More details on datasets and experiment settings, including hyperparameter values, are given in Appendices D.1 and D.2. The codebase is shared at `https://github.com/data-iitd/neutag`.

4.3 Baselines

We consider state-of-the-art graph transformers for comparison. We evaluate NEUTAG against GRAPHGPS (Rampášek et al., 2022) and its variant GRAPHGPS-GNN where we remove the GNN component to demonstrate the massive decrease in performance and henceforth dependency on MPNN. Similarly, we evaluate against EXPHORMER (Shirzad et al., 2023) and its variant EXPHORMER-GNN as well as GRIT (Ma et al., 2023), KAA (Fang et al., 2025),GRAPHORMER (Ying et al., 2021), NAGPHORMER (Chen et al., 2022b), GOAT (Kong et al., 2023) and LARGEGT (Dwivedi et al., 2023b).

Moreover, we further evaluate NEUTAG against standard and foundational graph neural networks GRAPH-SAGE (Hamilton et al., 2017), GAT (Veličković et al., 2018), GIN (Xu et al., 2019), LINKX (Lim et al., 2024) and MIXHOP (Abu-El-Haija et al., 2019). MIXHOP solves the over-smoothing in GNN while LINKX is a

Algorithm 1 NEUTAG Mini-batching algorithm

Require: $\mathcal{G}^{meta} = (\mathcal{V}^{meta} = \mathcal{V} \cup \mathcal{V}^f, \mathcal{E}^{meta} = \mathcal{E} \cup \mathcal{E}^f)$, # of layers L, Node feature matrix $\mathbf{X}$
Ensure: Sampled mini batch $\mathcal{G}^{meta'}$

$\mathcal{V}^{meta'} = \{\}$
$\mathcal{E}^{meta'} = \{\}$
{Sample a L hop subgraph from each feature node. This step can be cached as well as it will remain same across all batches}
for $v^f \in \mathcal{V}^f$ **do**
  $\mathcal{V}^{sampled} \sim$ 1-HOP$(\mathcal{G} = (\mathcal{V}, \mathcal{E}^f), v^f)$
  $(\mathcal{V}^L, \mathcal{E}^L) \sim$ L-HOP$(\mathcal{G} = (\mathcal{V}, \mathcal{E}), \mathcal{V}^{sampled})$
  $\mathcal{V}^{meta'} \leftarrow \mathcal{V}^{meta'} \cup \mathcal{V}^L$
  $\mathcal{E}^{meta'} \leftarrow \mathcal{E}^{meta'} \cup \mathcal{E}^L$
  for $v \in \mathcal{V}^{sampled}$ **do**
    $\mathcal{E}^{meta'} \leftarrow \mathcal{E}^{meta'} \cup (v, v^f)$
  end for
  $\mathcal{V}^{meta'} \leftarrow \mathcal{V}^{meta'} \cup v^f$
end for
{Sample a batch of original graph nodes and their L hop neighbors}
$\mathcal{V}' \sim \mathcal{V}$
for $v \in \mathcal{V}'$ **do**
  $(\mathcal{V}^L, \mathcal{E}^L) \sim$ L-HOP$(\mathcal{G} = (\mathcal{V}, \mathcal{E}), v)$
  $\mathcal{V}^{meta'} \leftarrow \mathcal{V}^{meta'} \cup \mathcal{V}^L$
  $\mathcal{E}^{meta'} \leftarrow \mathcal{E}^{meta'} \cup \mathcal{E}^L$
end for
{Sample feature nodes and edges for sampled graph nodes to create a mini-batch for forward propagation}

for $v \in \mathcal{V}^{meta'}$ **do**
  if $v \in \mathcal{V}$ **then**
    $\mathcal{E}^{meta'} \leftarrow \mathcal{E}^{meta'} \cup \{(v, f) \mid f \in \mathcal{V}^f, \mathbf{X}[v, f] = 1\}$
  end if
end for
Return $\mathcal{G}^{meta'} = (\mathcal{V}^{meta'}, \mathcal{E}^{meta'})$

Table 1: Comparison of NEUTAG against baseline GT on node classification task

Method	Cora	CiteSeer	Actor	Chameleon	OGBN-Arxiv	OGBN-Arxiv(Year)	Snap-patents
GRAPHGPS	83.65 ± 2.67	76.25 ± 1.34	34.30 ± 0.45	42.87 ± 1.88	OOM	OOM	OOM
GRAPHGPS-GNN	72.47 ± 1.87	71.59 ± 2.43	37.10 ± 1.11	47.36 ± 2.22	OOM	OOM	OOM
EXPHORMER	86.48 ± 2.15	75.92 ± 1.88	35.19 ± 0.94	45.17 ± 2.56	OOM	OOM	OOM
EXPHORMER-GNN	82.35 ± 1.75	73.01 ± 1.20	35.44 ± 0.86	46.97 ± 0.95	OOM	OOM	OOM
GRIT	82.56 ± 1.80	76.10 ± 0.67	35.34 ± 0.76	48.81 ± 2.26	OOM	OOM	OOM
GRAPHORMER	39.45 ± 10.66	OOM	OOM	26.89 ± 7.25	OOM	OOM	OOM
KAA	82.16 ± 1.36	71.83 ± 1.51	34.88 ± 0.89	45.44 ± 5.61	OOM	OOM	OOM
NAGPHORMER	86.78 ± 0.77	74.69 ± 1.06	33.03 ± 0.75	59.97 ± 1.72	67.36 ± 0.12	48.98 ± 0.23	61.27 ± 0.13
GOAT	84.93 ± 0.51	76.75 ± 1.84	$\mathbf{37.98 \pm 1.02}$	53.28 ± 2.48	$\mathbf{72.17 \pm 0.09}$	50.81 ± 0.36	55.35 ± 2.24
LARGEGT	83.42 ± 1.21	70.78 ± 1.62	37.47 ± 1.62	57.19 ± 1.89	67.56 ± 0.20	53.46 ± 0.78	$\mathbf{63.15 \pm 0.002}$
NEUTAG	$\mathbf{87.67 \pm 1.10}$	$\mathbf{77.68 \pm 1.90}$	36.21 ± 1.2	$\mathbf{65.26 \pm 2.43}$	70.63 ± 0.29	$\mathbf{53.96 \pm 0.38}$	63.00 ± 0.22

strong benchmark method for non-homophilic graphs. There exist multiple complementing techniques which enhance GNN performance, e.g., label-propagation (Huang et al., 2021), adaptive channel mixing (Luan et al., 2024b), gradient-gating (Rusch et al., 2023), data-augmentation (Zhao et al., 2022), (Chowdhury et al., 2023) and knowledge-distillation (Hong et al., 2024). Although these techniques can potentially affect GT architectures, study of their effects is beyond the scope of this paper, and we leave it for future work.

For completeness, we also compare NEUTAG with alternative attention formulations in graph transformers, specifically DIFFORMER (Wu et al., 2023a),SGFORMER (Wu et al., 2023b), POLYNORMER (Deng et al.,

2024), and AdvDIFFormer (Wu et al., 2025). These methods provide equivalent attention formulations that are complementary to sparse graph transformers and can potentially be integrated with Neutag and other baselines Goat, NagPhormer, GraphGPS, Exphormer, and LargeGT. Moreover, as discussed in the related work section 1.1, there exists a plethora of work focusing on improving positional and structural encodings, tokenization strategies, or other orthogonal design aspects, which are beyond the scope of this study.

4.4 Result Analysis

Comparison with Graph Transformers: Table 1 presents the node classification accuracy of baselines and the proposed model Neutag against 7 diverse datasets. The results clearly demonstrate the strong performance of the proposed model Neutag with respect to baselines. As we outlined in the introduction, while GraphGPS and Exphormer perform well on homophilic datasets, their performance drastically deteriorates after removing the Gnn component (-Gnn), which improves their performance on heterophilic graphs. Moreover, neither method is scalable for large-scale datasets. The recently proposed graph transformers Goat, NagPhormer, and LargeGT are scalable via global nodes; their performance is inconsistent across all graphs. E.g., Goat doesn't perform well on Cora, Chameleon, OGBN-Arxiv(year), and Snap-patents while good on CiteSeer, OGBN-Arxiv, and Actor. LargeGT is overall worse on small-scale graphs but delivers good performance on large-scale datasets. To further validate the effectiveness of Neutag, we extend our comparison with these scalable graph transformers in table 7 in the appendix to 5 additional small but challenging heterophilic datasets as defined in the survey (Luan et al., 2024a). Table 7 clearly demonstrates the strong performance of Neutag across these challenging heterophilic graphs. While no model outperforms all baselines across all datasets due to diverse inductive biases, our proposed data-agnostic sparse GT model Neutag adapts well to miscellaneous graphs, which is further supported by an analysis of the relative contributions of structural and feature-based attention paths (Appendix E.6). Neutag delivers stable performance, consistently ranking best or within 1.5% of the top model across all datasets.

Comparison with alternate attentions: Table 3 compares Neutag against alternative attention-based graph transformers, including DIFFormer, SGFormer, and Polynormer. DIFFormer has two variants: DIFFormer-s and DIFFormer-a, where the latter employs a non-linear kernel but fails to scale on medium-sized graphs. Neither variant is able to scale to large graphs like snap-patents. Among these baselines, Polynormer performs competitively with Neutag. However, both SGFormer and Polynormer require partitioning of large graphs into smaller subgraphs, leading to suboptimal results due to limited information exchange in case of snap-patent, unlike sparse GT Neutag, which utilizes information exchange between all nodes through its novel propagation framework. We note that these alternative attention mechanisms can be integrated into Neutag and other sparse GT baselines to enhance their performance, which we leave for future work.

Comparison with Graph Neural Networks: Table 2 presents the performance of Neutag against foundational Gnn on 7 datasets. Since information propagation in Gnn is limited to a few hops, we clearly see that they are competitive with Neutag only on homophilic graphs, Cora, and CiteSeer. Consequently, Gnn exhibits worse performance than Neutag on Chameleon, OGBN-Arxiv(year), and snap-patents, which require long-range interactions. This clearly establishes the necessity for information propagation from distant nodes for an optimal node classification model. Out of baselines, GraphSage and MixHop are consistent performers. Since MixHop utilizes a normalized Laplacian matrix, it doesn't scale to large graphs.

Table 2: Comparison of Neutag with Gnn on node classification task

Method	Cora	CiteSeer	Actor	Chameleon	OGBN-Arxiv	OGBN-Arxiv(Year)	Snap-patents
GraphSage	87.31 ± 0.96	76.55 ± 1.78	34.74 ± 1.20	48.95 ± 3.16	61.71 ± 0.79	46.34 ± 0.25	49.04 ± 0.03
Gat	86.56 ± 1.13	76.43 ± 2.55	30.03 ± 0.67	44.74 ± 3.29	62.35 ± 0.20	44.62 ± 0.52	36.64 ± 0.53
Gin	84.39 ± 0.65	75.47 ± 1.28	26.24 ± 0.52	32.68 ± 3.68	59.35 ± 0.30	46.60 ± 0.29	47.61 ± 0.12
MixHop	87.65 ± 0.20	76.97 ± 0.99	35.03 ± 0.53	47.68 ± 2.89	62.79 ± 0.39	44.80 ± 0.17	OOM
Linkx	83.14 ± 1.62	73.72 ± 0.14	32.78 ± 0.17	48.20 ± 3.31	60.39 ± 0.32	49.00 ± 0.39	52.71 ± 0.19
Neutag	$\mathbf{87.67 \pm 1.10}$	$\mathbf{77.68 \pm 1.90}$	$\mathbf{36.21 \pm 1.2}$	$\mathbf{65.26 \pm 2.43}$	70.63 ± 0.29	$\mathbf{53.96 \pm 0.38}$	$\mathbf{63.00 \pm 0.22}$

Table 3: Comparison of NEUTAG against alternate attention formulation based GT

Method	Cora	CiteSeer	Actor	Chameleon	OGBN-Arxiv	OGBN-Arxiv(year)	Snap-patents	Average
DIFFORMER-s	87.34 ± 1.52	$\mathbf{77.75 \pm 2.76}$	31.20 ± 0.81	57.41 ± 2.41	40.45 ± 1.69	36.74 ± 0.43	OOM	NA
DIFFORMER-a	86.01 ± 2.28	76.70 ± 1.95	30.79 ± 1.13	58.07 ± 1.95	OOM	OOM	OOM	NA
SGFORMER	86 ± 1.76	75.83 ± 2.28	31.03 ± 2.99	65.77 ± 1.68	74.51 ± 0.31	49.14 ± 0.34	29.44 ± 0.84	59.03
POLYNORMER	87.49 ± 1.01	75.62 ± 0.92	$\mathbf{37.22 \pm 1.60}$	$\mathbf{67.63 \pm 1.65}$	$\mathbf{74.85 \pm 0.15}$	52.12 ± 0.31	31.99 ± 0.24	60.98
POLYNORMER (-GNN)	71.66 ± 0.65	70.90 ± 1.20	38.16 ± 1.12	49.39 ± 1.69	65.84 ± 0.35	43.04 ± 0.18	31.10 ± 0.90	52.87
ADVDIFFORMER	79.08 ± 1.30	69.58 ± 1.95	33.30 ± 0.89	50.48 ± 5.13	66.83 ± 0.13	39.26 ± 0.58	OOM	NA
NEUTAG	$\mathbf{87.67 \pm 1.10}$	77.68 ± 1.90	36.21 ± 1.2	65.26 ± 2.43	70.63 ± 0.29	$\mathbf{53.96 \pm 0.38}$	$\mathbf{63.00 \pm 0.22}$	**64.91**

LINKX designed for heterophilic graphs is competitive on Chameleon and outperforms the rest of the GNN on large-scale snap-patent.

Scalability: As shown in Table 1, dense-attention-based GT models such as GRAPHGPS, EXPHORMER, and GRAPHORMER do not scale to large datasets such as OGBN-Arxiv, OGBN-Arxiv(year), and Snap-patents due to their computational and memory requirements. In contrast, scalable graph transformers such as NAGPHORMER, GOAT, and LARGEGT, along with our proposed method NEUTAG, can handle large-scale graphs. We provide additional analysis of training time and model size in Tables 11 and 12 (Appendix E.4). While NEUTAG is not the fastest or most lightweight among scalable methods, it achieves consistent performance across diverse settings, including both small- and large-scale datasets, and homophilic and heterophilic graphs, whereas none of these baselines do.

Ablation Study: We refer readers to the Appendix E.1 and E.7 to analyze the impact of various attention components and hyper-parameters in NEUTAG. Additionally, we conduct studies to understand the impact of missing features on the performance of NEUTAG in Appendix E.3.

5 Limitations

The major limitation of our work is that the proposed NEUTAG is not applicable to non-attributed graphs.

Moreover, the proposed method is specifically designed for node classification tasks in both small and large-scale graphs. In contrast, graph classification tasks involve small graphs, e.g., pattern, cluster, zinc, peptides-func, peptides-struct (Dwivedi et al., 2023a; 2022b), having around 100 nodes on average. In such cases, dense GT has shown to perform well without any computational challenges (Rampášek et al., 2022; Shirzad et al., 2023; Ying et al., 2021; Ma et al., 2023).

6 Conclusion

We introduced NEUTAG, a novel sparse graph transformer that unifies structural and feature information within a single attention mechanism. Unlike prior approaches relying on separate GNN components or virtual nodes, NEUTAG leverages features as global nodes, enabling long-range connectivity on attributed graphs. We further provide theoretical analysis on NEUTAG's capabilities. Finally, experiments on seven real-world datasets demonstrate that NEUTAG achieves competitive and consistent performance across diverse graph types, underlining its generality.

References

Sami Abu-El-Haija, Bryan Perozzi, Amol Kapoor, Nazanin Alipourfard, Kristina Lerman, Hrayr Harutyunyan, Greg Ver Steeg, and Aram Galstyan. MixHop: Higher-order graph convolutional architectures via sparsified neighborhood mixing. In Kamalika Chaudhuri and Ruslan Salakhutdinov (eds.), *Proceedings of the 36th International Conference on Machine Learning*, volume 97 of *Proceedings of Machine Learning Research*, pp. 21–29. PMLR, 09–15 Jun 2019. URL `https://proceedings.mlr.press/v97/abu-el-haija19a.html`.

Reid Andersen, Fan Chung, and Kevin Lang. Local graph partitioning using pagerank vectors. In *2006 47th Annual IEEE Symposium on Foundations of Computer Science (FOCS'06)*, pp. 475–486. IEEE, 2006.

Jimmy Lei Ba, Jamie Ryan Kiros, and Geoffrey E. Hinton. Layer normalization, 2016.

Ravinder Bhattoo, Sayan Ranu, and NM Krishnan. Learning articulated rigid body dynamics with lagrangian graph neural network. *Advances in Neural Information Processing Systems*, 35:29789–29800, 2022.

Vaibhav Bihani, Sahil Manchanda, Srikanth Sastry, Sayan Ranu, and NM Krishnan. Stridernet: A graph reinforcement learning approach to optimize atomic structures on rough energy landscapes. In *ICML*, 2023.

Suresh Bishnoi, Ravinder Bhattoo, Sayan Ranu, and NM Krishnan. Enhancing the inductive biases of graph neural ode for modeling dynamical systems. *ICLR*, 2023.

Suresh Bishnoi, Jayadeva Jayadeva, Sayan Ranu, and NM Anoop Krishnan. Brognet: Momentum-conserving graph neural stochastic differential equation for learning brownian dynamics. In *The Twelfth International Conference on Learning Representations*, 2024.

Giorgos Bouritsas, Fabrizio Frasca, Stefanos Zafeiriou, and Michael M. Bronstein. Improving graph neural network expressivity via subgraph isomorphism counting, 2021. URL `https://openreview.net/forum?id=LT0KSFnQDWF`.

Chen Cai, Truong Son Hy, Rose Yu, and Yusu Wang. On the connection between mpnn and graph transformer. In *International Conference on Machine Learning*, pp. 3408–3430. PMLR, 2023.

Deli Chen, Yankai Lin, Wei Li, Peng Li, Jie Zhou, and Xu Sun. Measuring and relieving the over-smoothing problem for graph neural networks from the topological view. *Proceedings of the AAAI Conference on Artificial Intelligence*, 34(04):3438–3445, Apr. 2020. doi: 10.1609/aaai.v34i04.5747. URL `https://ojs.aaai.org/index.php/AAAI/article/view/5747`.

Dexiong Chen, Leslie O'Bray, and Karsten Borgwardt. Structure-aware transformer for graph representation learning. In *Proceedings of the 39th International Conference on Machine Learning (ICML)*, Proceedings of Machine Learning Research, 2022a.

Jinsong Chen, Kaiyuan Gao, Gaichao Li, and Kun He. Nagphormer: A tokenized graph transformer for node classification in large graphs. *arXiv preprint arXiv:2206.04910*, 2022b.

Krzysztof Choromanski, Valerii Likhosherstov, David Dohan, Xingyou Song, Andreea Gane, Tamas Sarlos, Peter Hawkins, Jared Davis, Afroz Mohiuddin, Lukasz Kaiser, et al. Rethinking attention with performers. *arXiv preprint arXiv:2009.14794*, 2020.

Anjan Chowdhury, Sriram Srinivasan, Animesh Mukherjee, Sanjukta Bhowmick, and Kuntal Ghosh. Improving node classification accuracy of gnn through input and output intervention. *ACM Trans. Knowl. Discov. Data*, 18(1), sep 2023. ISSN 1556-4681. doi: 10.1145/3610535. URL `https://doi.org/10.1145/3610535`.

Chenhui Deng, Zichao Yue, and Zhiru Zhang. Polynormer: Polynomial-expressive graph transformer in linear time. In *The Twelfth International Conference on Learning Representations*, 2024. URL `https://openreview.net/forum?id=hmv1LpNfXa`.

Jacob Devlin, Ming-Wei Chang, Kenton Lee, and Kristina Toutanova. Bert: Pre-training of deep bidirectional transformers for language understanding, 2019.

Rahul Dey and Fathi M Salem. Gate-variants of gated recurrent unit (gru) neural networks. In *2017 IEEE 60th international midwest symposium on circuits and systems (MWSCAS)*, pp. 1597–1600. IEEE, 2017.

Alexey Dosovitskiy, Lucas Beyer, Alexander Kolesnikov, Dirk Weissenborn, Xiaohua Zhai, Thomas Unterthiner, Mostafa Dehghani, Matthias Minderer, Georg Heigold, Sylvain Gelly, et al. An image is worth 16x16 words: Transformers for image recognition at scale. *arXiv preprint arXiv:2010.11929*, 2020.

Vijay Prakash Dwivedi and Xavier Bresson. A generalization of transformer networks to graphs, 2021. URL `https://arxiv.org/abs/2012.09699`.

Vijay Prakash Dwivedi, Anh Tuan Luu, Thomas Laurent, Yoshua Bengio, and Xavier Bresson. Graph neural networks with learnable structural and positional representations. In *International Conference on Learning Representations*, 2022a. URL `https://openreview.net/forum?id=wTTjnvGphYj`.

Vijay Prakash Dwivedi, Ladislav Rampášek, Mikhail Galkin, Ali Parviz, Guy Wolf, Anh Tuan Luu, and Dominique Beaini. Long range graph benchmark. In *Proceedings of the 36th International Conference on Neural Information Processing Systems*, NIPS '22, Red Hook, NY, USA, 2022b. Curran Associates Inc. ISBN 9781713871088.

Vijay Prakash Dwivedi, Chaitanya K Joshi, Anh Tuan Luu, Thomas Laurent, Yoshua Bengio, and Xavier Bresson. Benchmarking graph neural networks. *Journal of Machine Learning Research*, 24(43):1–48, 2023a.

Vijay Prakash Dwivedi, Yozen Liu, Anh Tuan Luu, Xavier Bresson, Neil Shah, and Tong Zhao. Graph transformers for large graphs, 2023b.

Taoran Fang, Tianhong Gao, Chunping Wang, Yihao Shang, Wei Chow, Lei Chen, and Yang Yang. Kaa: Kolmogorov-arnold attention for enhancing attentive graph neural networks. In *International Conference on Learning Representations*, 2025.

Fabian B. Fuchs, Daniel E. Worrall, Volker Fischer, and Max Welling. Se(3)-transformers: 3d roto-translation equivariant attention networks. In *Proceedings of the 34th International Conference on Neural Information Processing Systems*, NIPS '20, Red Hook, NY, USA, 2020. Curran Associates Inc. ISBN 9781713829546.

Fabian B. Fuchs, Edward Wagstaff, Justas Dauparas, and Ingmar Posner. Iterative se(3)-transformers, 2021. URL `https://arxiv.org/abs/2102.13419`.

Nikhil Goyal, Harsh Vardhan Jain, and Sayan Ranu. Graphgen: a scalable approach to domain-agnostic labeled graph generation. In *Proceedings of The Web Conference 2020*, pp. 1253–1263, 2020.

Anjali Gupta, Prashant Kumar, Aniket Mishra, Abhishek Singh, Surender Kumar, Muthusamy Chelliah, Abhijnan Chakraborty, and Sayan Ranu. Persona identification in e-commerce with scarce labels and in-context graph learning. In *Proceedings of the 31st ACM SIGKDD Conference on Knowledge Discovery and Data Mining V. 2*, pp. 778–789, 2025.

Mridul Gupta, Hariprasad Kodamana, and Sayan Ranu. FRIGATE: Frugal spatio-temporal forecasting on road networks. In *29th SIGKDD Conference on Knowledge Discovery and Data Mining*, 2023. URL `https://openreview.net/forum?id=2cTw2M47L1`.

Will Hamilton, Zhitao Ying, and Jure Leskovec. Inductive representation learning on large graphs. *Advances in neural information processing systems*, 30, 2017.

Kaiming He, Xiangyu Zhang, Shaoqing Ren, and Jian Sun. Deep residual learning for image recognition. In *Proceedings of the IEEE conference on computer vision and pattern recognition*, pp. 770–778, 2016.

Geoffrey Hinton, Oriol Vinyals, and Jeff Dean. Distilling the knowledge in a neural network, 2015. URL `https://arxiv.org/abs/1503.02531`.

Xiaobin Hong, Wenzhong Li, Chaoqun Wang, Mingkai Lin, and Sanglu Lu. Label attentive distillation for gnn-based graph classification. *Proceedings of the AAAI Conference on Artificial Intelligence*, 38(8): 8499–8507, Mar. 2024. doi: 10.1609/aaai.v38i8.28693. URL `https://ojs.aaai.org/index.php/AAAI/article/view/28693`.

Weihua Hu, Matthias Fey, Marinka Zitnik, Yuxiao Dong, Hongyu Ren, Bowen Liu, Michele Catasta, and Jure Leskovec. Open graph benchmark: datasets for machine learning on graphs. In *Proceedings of the 34th International Conference on Neural Information Processing Systems*, NIPS '20, Red Hook, NY, USA, 2020. Curran Associates Inc. ISBN 9781713829546.

Qian Huang, Horace He, Abhay Singh, Ser-Nam Lim, and Austin R. Benson. Combining label propagation and simple models out-performs graph neural networks. In *9th International Conference on Learning Representations, ICLR 2021, Virtual Event, Austria, May 3-7, 2021*. OpenReview.net, 2021. URL `https://openreview.net/forum?id=8E1-f3VhX1o`.

Md Shamim Hussain, Mohammed J. Zaki, and Dharmashankar Subramanian. Global self-attention as a replacement for graph convolution. In *Proceedings of the 28th ACM SIGKDD Conference on Knowledge Discovery and Data Mining*, KDD '22, pp. 655–665, New York, NY, USA, 2022. Association for Computing Machinery. ISBN 9781450393850. doi: 10.1145/3534678.3539296. URL https://doi.org/10.1145/3534678.3539296.

Sergey Ioffe and Christian Szegedy. Batch normalization: Accelerating deep network training by reducing internal covariate shift, 2015.

Jayant Jain, Vrittika Bagadia, Sahil Manchanda, and Sayan Ranu. Neuromlr: Robust & reliable route recommendation on road networks. *Advances in Neural Information Processing Systems*, 34:22070–22082, 2021.

Jinwoo Kim, Dat Tien Nguyen, Seonwoo Min, Sungjun Cho, Moontae Lee, Honglak Lee, and Seunghoon Hong. Pure transformers are powerful graph learners. In Alice H. Oh, Alekh Agarwal, Danielle Belgrave, and Kyunghyun Cho (eds.), *Advances in Neural Information Processing Systems*, 2022. URL https://openreview.net/forum?id=um2BxfgkT2_.

Thomas N. Kipf and Max Welling. Semi-supervised classification with graph convolutional networks. In *International Conference on Learning Representations (ICLR)*, 2017.

Kezhi Kong, Jiuhai Chen, John Kirchenbauer, Renkun Ni, C Bayan Bruss, and Tom Goldstein. Goat: A global transformer on large-scale graphs. In *International Conference on Machine Learning*, pp. 17375–17390. PMLR, 2023.

Devin Kreuzer, Dominique Beaini, Will Hamilton, Vincent Létourneau, and Prudencio Tossou. Rethinking graph transformers with spectral attention. *Advances in Neural Information Processing Systems*, 34: 21618–21629, 2021a.

Devin Kreuzer, Dominique Beaini, William L. Hamilton, Vincent Létourneau, and Prudencio Tossou. Rethinking graph transformers with spectral attention. In *Proceedings of the 35th International Conference on Neural Information Processing Systems*, NIPS '21, Red Hook, NY, USA, 2021b. Curran Associates Inc. ISBN 9781713845393.

Weirui Kuang, WANG Zhen, Yaliang Li, Zhewei Wei, and Bolin Ding. Coarformer: Transformer for large graph via graph coarsening. 2021.

Derek Lim, Felix Hohne, Xiuyu Li, Sijia Linda Huang, Vaishnavi Gupta, Omkar Bhalerao, and Ser Nam Lim. Large scale learning on non-homophilous graphs: New benchmarks and strong simple methods. In M. Ranzato, A. Beygelzimer, Y. Dauphin, P.S. Liang, and J. Wortman Vaughan (eds.), *Advances in Neural Information Processing Systems*, volume 34, pp. 20887–20902. Curran Associates, Inc., 2021. URL https://proceedings.neurips.cc/paper_files/paper/2021/file/ae816a80e4c1c56caa2eb4e1819cbb2f-Paper.pdf.

Derek Lim, Joshua David Robinson, Lingxiao Zhao, Tess Smidt, Suvrit Sra, Haggai Maron, and Stefanie Jegelka. Sign and basis invariant networks for spectral graph representation learning. In *The Eleventh International Conference on Learning Representations*, 2023. URL https://openreview.net/forum?id=Q-UHqMorzil.

Derek Lim, Felix Hohne, Xiuyu Li, Sijia Linda Huang, Vaishnavi Gupta, Omkar Bhalerao, and Ser-Nam Lim. Large scale learning on non-homophilous graphs: new benchmarks and strong simple methods. In *Proceedings of the 35th International Conference on Neural Information Processing Systems*, NIPS '21, Red Hook, NY, USA, 2024. Curran Associates Inc. ISBN 9781713845393.

Chuang Liu, Yibing Zhan, Xueqi Ma, Liang Ding, Dapeng Tao, Jia Wu, and Wenbin Hu. Gapformer: Graph transformer with graph pooling for node classification. In *IJCAI*, pp. 2196–2205, 2023.

Meng Liu, Hongyang Gao, and Shuiwang Ji. Towards deeper graph neural networks. In *Proceedings of the 26th ACM SIGKDD International Conference on Knowledge Discovery & Data Mining*, KDD '20, pp. 338–348, New York, NY, USA, 2020. Association for Computing Machinery. ISBN 9781450379984. doi: 10.1145/3394486.3403076. URL https://doi.org/10.1145/3394486.3403076.

Sitao Luan, Chenqing Hua, Qincheng Lu, Liheng Ma, Lirong Wu, Xinyu Wang, Minkai Xu, Xiao-Wen Chang, Doina Precup, Rex Ying, Stan Z. Li, Jian Tang, Guy Wolf, and Stefanie Jegelka. The heterophilic graph learning handbook: Benchmarks, models, theoretical analysis, applications and challenges, 2024a. URL https://arxiv.org/abs/2407.09618.

Sitao Luan, Chenqing Hua, Qincheng Lu, Jiaqi Zhu, Mingde Zhao, Shuyuan Zhang, Xiao-Wen Chang, and Doina Precup. Revisiting heterophily for graph neural networks. In *Proceedings of the 36th International Conference on Neural Information Processing Systems*, NIPS '22, Red Hook, NY, USA, 2024b. Curran Associates Inc. ISBN 9781713871088.

Shengjie Luo, Tianlang Chen, Yixian Xu, Shuxin Zheng, Tie-Yan Liu, Liwei Wang, and Di He. One transformer can understand both 2d & 3d molecular data, 2023. URL https://arxiv.org/abs/2210.01765.

Liheng Ma, Chen Lin, Derek Lim, Adriana Romero-Soriano, Puneet K. Dokania, Mark Coates, Philip H.S. Torr, and Ser-Nam Lim. Graph inductive biases in transformers without message passing. In *Proceedings of the 40th International Conference on Machine Learning*, ICML'23. JMLR.org, 2023.

Alireza Makhzani and Brendan J. Frey. k-sparse autoencoders. *CoRR*, abs/1312.5663, 2013. URL https://api.semanticscholar.org/CorpusID:14850799.

Luis Müller, Mikhail Galkin, Christopher Morris, and Ladislav Rampášek. Attending to graph transformers. *Transactions on Machine Learning Research*, 2024. ISSN 2835-8856. URL https://openreview.net/forum?id=HhbqHBBrfZ.

Sunil Nishad, Shubhangi Agarwal, Arnab Bhattacharya, and Sayan Ranu. Graphreach: Position-aware graph neural network using reachability estimations. *IJCAI*, 2021.

Kenta Oono and Taiji Suzuki. Graph neural networks exponentially lose expressive power for node classification. *ICLR2020*, 8, 2020.

Lawrence Page, Sergey Brin, Rajeev Motwani, and Terry Winograd. The pagerank citation ranking : Bringing order to the web. In *The Web Conference*, 1999. URL https://api.semanticscholar.org/CorpusID:1508503.

Hongbin Pei, Bingzhe Wei, Kevin Chen-Chuan Chang, Yu Lei, and Bo Yang. Geom-gcn: Geometric graph convolutional networks. In *8th International Conference on Learning Representations, ICLR 2020, Addis Ababa, Ethiopia, April 26-30, 2020*. OpenReview.net, 2020. URL https://openreview.net/forum?id=S1e2agrFvS.

Alec Radford, Jeff Wu, Rewon Child, David Luan, Dario Amodei, and Ilya Sutskever. Language models are unsupervised multitask learners. 2019. URL https://api.semanticscholar.org/CorpusID:160025533.

Ladislav Rampášek, Mikhail Galkin, Vijay Prakash Dwivedi, Anh Tuan Luu, Guy Wolf, and Dominique Beaini. Recipe for a General, Powerful, Scalable Graph Transformer. *Advances in Neural Information Processing Systems*, 35, 2022.

Benedek Rozemberczki, Carl Allen, and Rik Sarkar. Multi-scale attributed node embedding. *Journal of Complex Networks*, 9(2):cnab014, 2021.

T Konstantin Rusch, Benjamin Paul Chamberlain, Michael W Mahoney, Michael M Bronstein, and Siddhartha Mishra. Gradient gating for deep multi-rate learning on graphs. *ICLR*, 9:25, 2023.

Nimrod Segol and Yaron Lipman. On universal equivariant set networks. In *International Conference on Learning Representations*, 2019.

Prithviraj Sen, Galileo Namata, Mustafa Bilgic, Lise Getoor, Brian Galligher, and Tina Eliassi-Rad. Collective classification in network data. *AI Magazine*, 29(3):93, Sep. 2008. doi: 10.1609/aimag.v29i3.2157. URL https://ojs.aaai.org/index.php/aimagazine/article/view/2157.

Yu Shi, Shuxin Zheng, Guolin Ke, Yifei Shen, Jiacheng You, Jiyan He, Shengjie Luo, Chang Liu, Di He, and Tie-Yan Liu. Benchmarking graphormer on large-scale molecular modeling datasets, 2023. URL https://arxiv.org/abs/2203.04810.

Hamed Shirzad, Ameya Velingker, Balaji Venkatachalam, Danica J Sutherland, and Ali Kemal Sinop. Exphormer: Sparse transformers for graphs. In *International Conference on Machine Learning*, pp. 31613–31632. PMLR, 2023.

Anuj Kumar Sirohi, Anjali Gupta, Sandeep Kumar, Amitabha Bagchi, and Sayan Ranu. Graphgini: Fostering individual and group fairness in graph neural networks. *arXiv preprint arXiv:2402.12937*, 2024.

Ashish Vaswani, Noam Shazeer, Niki Parmar, Jakob Uszkoreit, Llion Jones, Aidan N Gomez, Ł ukasz Kaiser, and Illia Polosukhin. Attention is all you need. In I. Guyon, U. Von Luxburg, S. Bengio, H. Wallach, R. Fergus, S. Vishwanathan, and R. Garnett (eds.), *Advances in Neural Information Processing Systems*, volume 30. Curran Associates, Inc., 2017. URL https://proceedings.neurips.cc/paper_files/paper/2017/file/3f5ee243547dee91fbd053c1c4a845aa-Paper.pdf.

Petar Veličković, Guillem Cucurull, Arantxa Casanova, Adriana Romero, Pietro Liò, and Yoshua Bengio. Graph Attention Networks. *International Conference on Learning Representations*, 2018. URL https://openreview.net/forum?id=rJXMpikCZ.

Haorui Wang, Haoteng Yin, Muhan Zhang, and Pan Li. Equivariant and stable positional encoding for more powerful graph neural networks. In *International Conference on Learning Representations*, 2022. URL https://openreview.net/forum?id=e95i1IHcWj.

Qitian Wu, Chenxiao Yang, Wentao Zhao, Yixuan He, David Wipf, and Junchi Yan. DIFFormer: Scalable (graph) transformers induced by energy constrained diffusion. In *The Eleventh International Conference on Learning Representations*, 2023a. URL https://openreview.net/forum?id=j6zUzrapY3L.

Qitian Wu, Wentao Zhao, Chenxiao Yang, Hengrui Zhang, Fan Nie, Haitian Jiang, Yatao Bian, and Junchi Yan. Simplifying and empowering transformers for large-graph representations. In *Thirty-seventh Conference on Neural Information Processing Systems*, 2023b. URL https://openreview.net/forum?id=R4xpvDTWkV.

Qitian Wu, Chenxiao Yang, Kaipeng Zeng, and Michael M. Bronstein. Supercharging graph transformers with advective diffusion. In *Forty-second International Conference on Machine Learning*, 2025. URL https://openreview.net/forum?id=MaOYl3P84E.

Keyulu Xu, Weihua Hu, Jure Leskovec, and Stefanie Jegelka. How powerful are graph neural networks? In *International Conference on Learning Representations*, 2019. URL https://openreview.net/forum?id=ryGs6iA5Km.

Zhilin Yang, William W. Cohen, and Ruslan Salakhutdinov. Revisiting semi-supervised learning with graph embeddings. In *Proceedings of the 33rd International Conference on International Conference on Machine Learning - Volume 48*, ICML'16, pp. 40–48. JMLR.org, 2016.

Chengxuan Ying, Tianle Cai, Shengjie Luo, Shuxin Zheng, Guolin Ke, Di He, Yanming Shen, and Tie-Yan Liu. Do transformers really perform badly for graph representation? In A. Beygelzimer, Y. Dauphin, P. Liang, and J. Wortman Vaughan (eds.), *Advances in Neural Information Processing Systems*, 2021. URL https://openreview.net/forum?id=OeWooOxFwDa.

Chulhee Yun, Srinadh Bhojanapalli, Ankit Singh Rawat, Sashank Reddi, and Sanjiv Kumar. Are transformers universal approximators of sequence-to-sequence functions? In *International Conference on Learning Representations*, 2020. URL https://openreview.net/forum?id=ByxRM0Ntvr.

Manzil Zaheer, Satwik Kottur, Siamak Ravanbakhsh, Barnabas Poczos, Russ R Salakhutdinov, and Alexander J Smola. Deep sets. *Advances in neural information processing systems*, 30, 2017.

Manzil Zaheer, Guru Guruganesh, Avinava Dubey, Joshua Ainslie, Chris Alberti, Santiago Ontanon, Philip Pham, Anirudh Ravula, Qifan Wang, Li Yang, and Amr Ahmed. Big bird: Transformers for longer sequences, 2021.

Tong Zhao, Xianfeng Tang, Danqing Zhang, Haoming Jiang, Nikhil Rao, Yiwei Song, Pallav Agrawal, Karthik Subbian, Bing Yin, and Meng Jiang. Autogda: Automated graph data augmentation for node classification. In Bastian Rieck and Razvan Pascanu (eds.), *Proceedings of the First Learning on Graphs Conference*, volume 198 of *Proceedings of Machine Learning Research*, pp. 32:1–32:17. PMLR, 09–12 Dec 2022. URL `https://proceedings.mlr.press/v198/zhao22a.html`.

Jiong Zhu, Yujun Yan, Lingxiao Zhao, Mark Heimann, Leman Akoglu, and Danai Koutra. Beyond homophily in graph neural networks: current limitations and effective designs. In *Proceedings of the 34th International Conference on Neural Information Processing Systems*, NIPS '20, Red Hook, NY, USA, 2020. Curran Associates Inc. ISBN 9781713829546.

Wenhao Zhu, Guojie Song, Liang Wang, and Shaoguo Liu. Anchorgt: Efficient and flexible attention architecture for scalable graph transformers. *arXiv preprint arXiv:2405.03481*, 2024.

A Preliminaries

Definition 1 (Graph). *A graph is defined as $\mathcal{G} = (\mathcal{V}, \mathcal{E}, \mathbf{X})$ over node and edge sets $\mathcal{V}$ and $\mathcal{E} = \{(u, v) \mid u, v \in \mathcal{V}\}$ respectively where $\mid \mathcal{V} \mid = N$ and $\mid \mathcal{E} \mid = M$. Edge set is also represented using an adjacency matrix $\mathcal{A} \in \{0, 1\}^{N \times N}$. $\mathbf{X} \in \{0, 1\}^{N \times F}$ is a node feature matrix where $\mathcal{F} = \bigcup_{v \in \mathcal{V}} \mathcal{F}_v$ is the set of all features in graph $\mathcal{G}$. $\mathcal{F}_v$ is a feature set at node v and $\mid \mathcal{F} \mid = F$.*

Problem 1 (Graph transformer for node classification).

Input: *Given a graph $\mathcal{G}$ (Def. 1), let $Y : \mathcal{V} \to \mathbb{R}$ be a hidden function that maps a node to a real number. $Y(v)$ is known to us only for the subset $\mathcal{V}_l \subset \mathcal{V}$ and may model some downstream tasks such as node classification or link prediction.*

Goal: *Learn parameters Θ of a Transformer based graph neural network, denoted as GT_Θ, that predicts $Y(v)$, $\forall v \in \mathcal{V}_l$ accurately.*

We now introduce preliminaries of Graph Neural Networks, Transformers, and Graph Transformers for node classification tasks.

A.1 Graph

Gnn also known as message-passing neural networks, as each node exchanges messages from its neighbors to compute its representation. These representations are utilized in downstream tasks such as node classification and link prediction. Though there exists more specialized Gnn for the link-prediction task that utilizes link-based features instead of node-level, those are out of scope in this work. State-of-the-art Gnn (Xu et al., 2019; Veličković et al., 2018; Hamilton et al., 2017) for node classification tasks follows the following framework. Assuming $\mathbf{x}_v \in \mathcal{R}^{|F|}$ as feature vector for node v, 0^{th} layer embedding is defined as:

$$\mathbf{h}_v^0 = \mathbf{x}_v \; \forall v \in \mathcal{V} \tag{18}$$

Next, l^{th} layer representation is computed using nodes' neighbourhood $\mathcal{N}_v = \{u \mid (u, v) \in \mathcal{E}\} \; \forall \; v \in \mathcal{V}$ as follows.

$$\mathbf{m}_v^l = \textsc{msg}(\mathbf{h}_u^{l-1}, \mathbf{h}_v^{l-1}) \forall u \in \mathcal{N}_v \tag{19}$$

Messages are computed from each neighbor using the previous layer information. This information is then aggregated at each node as follows.

$$\overline{\mathbf{m}}_v = \textsc{aggregate}^l(\{\!\{\mathbf{m}_v^l(u), \forall u \in \mathcal{N}_v\}\!\}) \tag{20}$$

Symbol	Meaning
$\mathcal{G}$	Input graph
$\mathcal{V}$	Set of nodes in $\mathcal{G}$
$\mathcal{E}$	Set of edges in $\mathcal{G}$
$\mathbf{X}$	Node feature matrix
$\mathcal{F}$	Set of features in $\mathcal{G}$
$\mathcal{G}^{meta}$	Transformed input graph
$\mathcal{V}^f$	Set of features as virtual node in $\mathcal{G}^{meta}$
$\mathcal{E}^f$	Set of edges between nodes and respective features $\mathcal{G}^{meta}$
$\mathcal{E}^{f-}$	Set of edges between nodes and absent features nodes in $\mathcal{G}^{meta}$
$\mathcal{V}^{meta}$	Set of nodes in $\mathcal{G}^{meta}$
$\mathcal{E}^{meta}$	Set of edges in $\mathcal{G}^{meta}$
$D^{\mathcal{G}}$	Average node degree excluding feature nodes in $\mathcal{G}^{meta}$
D^{F}	Average node degree excluding graph nodes in $\mathcal{G}^{meta}$
$y(v)$	Label of node v
$ppr_i^{\mathcal{G}}(v)$	i^{th} nearest node from node v sorted using personalized page rank score
$\mathbf{M}$	Projection matrix
$\mathbf{h}_i^l$	Embedding of node i at l^{th} layer
$\mathbf{H}_{\mathcal{V}}^l$	Embedding matrix of graph nodes $\mathcal{V}$ at layer l
$\mathbf{H}_{\mathcal{V}^f}^l$	Embedding matrix of feature nodes $\mathcal{V}^f$ at layer l
$\mathbf{W}$	Learnable weight matrices
$\mathbf{Q}_{\mathcal{V}}^l$	Query matrix at layer l for graph nodes $\mathcal{V}$
$\mathbf{K}_{\mathcal{V}}^l$	Key matrix at layer l for graph nodes $\mathcal{V}$
$\mathbf{V}_{\mathcal{V}}^l$	Value matrix at layer l for graph nodes $\mathcal{V}$
$\mathbf{Q}_{\mathcal{V}^f}^l$	Query matrix at layer l for feature nodes $\mathcal{V}^f$
$\mathbf{K}_{\mathcal{V}^f}^l$	Key matrix at layer l for feature nodes $\mathcal{V}^f$
$\mathbf{V}_{\mathcal{V}^f}^l$	Value matrix at layer l for feature nodes $\mathcal{V}^f$
$\mathcal{N}_v^{\mathcal{G}}$	Set of neighbors excluding feature nodes of node v in $\mathcal{G}^{meta}$
$\mathcal{N}_v^f$	Set of neighbors consisting of only feature nodes of node v in $\mathcal{G}^{meta}$
$\mathcal{N}_f^{\mathcal{G}}$	Set of neighbors excluding feature nodes of a feature node f in $\mathcal{G}^{meta}$

Table 4: Notations and their definition

$\{\!\{\ldots\}\!\}$ is a multi-set as the same message can arrive from multiple neighbors. Multi-set allows multiple instances of the same element achieving improved expressivity, highlighted in (Xu et al., 2019). Finally, the aggregated message and previous layer $l-1$ representation are combined to compute the l^{th} layer representation as follows.

$$\mathbf{h}_v^l = \textsc{combine}(\mathbf{h}_v^{l-1}, \overline{\mathbf{m}}_v) \tag{21}$$

where MSG, AGGREGATE and COMBINE are non-neural functions like SUM, AVERAGE or MAX-POOL or neural networks based learnable functions like *mlp*, *attention* (Vaswani et al., 2017) and *recurrent neural networks* eg. GRU (Dey & Salem, 2017). To achieve L hop deeper GNN, equations 19, 20 and 21 are applied L times successively to compute $\mathbf{h}_v^L$. This representation is utilized for node classification tasks. GNN are limited in modeling long-range dependencies as increasing the number of layers leads to *over-smoothing*(Oono & Suzuki, 2020; Chen et al., 2020) where node embeddings become approximately similar at every node. Graph Transformers solves this by introducing the mechanism of each node attending to all other nodes as follows.

A.2 Transformers

First, we define the transformer neural nets, the key components of graph transformers. Given a graph $\mathcal{G} = (\mathcal{V}, \mathcal{E}, \mathbf{X})$ and ignoring topological connections $\mathcal{E}$, contextualized node representations $\mathbf{H}^L$ are computed using self-attention. The representations are first initialized using node features.

$$\mathbf{H}^0 = \mathbf{X}\mathbf{W} \tag{22}$$

where $\mathbf{W}$ is the trainable weight matrix. Next, below equations 23 and 24 are repeated for $l \in [1 \dots L]$ as follows.

$$\mathbf{H}^l = \Big\|_{h=1}^{h=H} \textsc{softmax}\left(\frac{(\mathbf{H}^{l-1}\mathbf{W}_Q^h)(\mathbf{H}^{l-1}\mathbf{W}_K^h)^T}{\sqrt{d}}\right)\mathbf{H}^{l-1}\mathbf{W}_V^h \tag{23}$$

$$\mathbf{H}^l = \textsc{norm}(\mathbf{H}^{l-1} + \textsc{ffn}(\mathbf{H}^l)) \tag{24}$$

where NORM is either batch-norm (Ioffe & Szegedy, 2015) or layer-norm (Ba et al., 2016), FFN is feed-forward neural network. $\mathbf{W}_Q$, $\mathbf{W}_K$ and $\mathbf{W}_V$ are projection matrix $\in \mathcal{R}^{d \times d_k}$. H is a number of heads, and the transformer concatenates these multiple heads, facilitating diverse attention coefficients. This is also known as *Multi-head Attention*. This architecture uses skip-connections and activation norm strategies required in deeper neural networks (He et al., 2016).

A.3 Graph Transformers (GT)

Now, we discuss graph transformers, which incorporate graph topology $\mathcal{E}$ into the attention mechanism. Foremost, node attributes are combined with position encodings, e.g., Random walk-based encoding (Dwivedi et al., 2022a) and Laplacian eigenvalues (Dwivedi et al., 2023a) denoted as $\mathbf{PE}$ matrix.

$$\mathbf{H}^0 = (\mathbf{X} + \mathbf{PE})\mathbf{W} \tag{25}$$

Next, assuming we have node presentation for $l-1$ layer, it is passed to the GNN layer along with the transformer layer to compute l^{th} layer representation as follows.

$$\mathbf{H}^l_{gnn} = \textsc{gnn}(\mathbf{H}^{l-1}, \mathcal{E}) \tag{26}$$

$$\mathbf{H}^l_{T} = \textsc{transformer}(\mathbf{H}^{l-1}, \mathcal{E}) \tag{27}$$

where GNN is any graph neural network described earlier. TRANSFORMER layer can be defined as in current literature (Rampášek et al., 2022; Shirzad et al., 2023; Kong et al., 2023; Dwivedi et al., 2023b). Finally, the representation computed using GNN and TRANSFORMER are combined to learn l^{th} layer representation.

$$\mathbf{H}^l = \textsc{ffn}(\mathbf{H}^l_{gnn}, \mathbf{H}^l_T) \tag{28}$$

B Proof of Theorems

B.1 Connectivity Analysis of $\mathcal{G}^{meta}$: Proof of theorem 1

Proof: First, we define the number of 1-hop neighbors of the graph and feature nodes where $\#Nbrs(\mathcal{V}, l)$ signifies the order of l-hop neighbors of graph nodes $\mathcal{V}$ and $\#Nbrs(\mathcal{V}^f, l)$ is the order of number of l-hop neighbors of feature nodes $\mathcal{V}^f$.

$$\#Nbrs(\mathcal{V}, 1) = O(D^{\mathcal{G}} + D^F), \quad \#Nbrs(\mathcal{V}^f, 1) = O(F^{\mathcal{G}}) \tag{29}$$

As each D^F feature node will connect to graph nodes connected to it, and each graph node $F^{\mathcal{G}}$ and $D^{\mathcal{G}}$ will be connected to its neighbors and feature nodes, applying this for 2 hops,

$$\begin{aligned} \#Nbrs(\mathcal{V}, 2) &= O(D^{\mathcal{G}} * (D^{\mathcal{G}} + D^F) + D^F * F^{\mathcal{G}}), \\ \#Nbrs(\mathcal{V}^f, 2) &= O(F^{\mathcal{G}} * (D^{\mathcal{G}} + D^F)) \end{aligned} \tag{30}$$

$$\#Nbrs(\mathcal{V},3) = O(D^{\mathcal{G}} * (D^{\mathcal{G}} * (D^{\mathcal{G}} + D^F) + D^F * F^{\mathcal{G}}) + D^F * F^{\mathcal{G}} * (D^{\mathcal{G}} + D^F)) \tag{31}$$

$$\begin{aligned}\#Nbrs(\mathcal{V},4) =& O(D^{\mathcal{G}} * (D^{\mathcal{G}} * (D^{\mathcal{G}} * (D^{\mathcal{G}} + D^F) + D^F * F^{\mathcal{G}}) + D^F * F^{\mathcal{G}} * (D^{\mathcal{G}} + D^F)) \\ &+ D^F * F^{\mathcal{G}} * (D^{\mathcal{G}} * (D^{\mathcal{G}} + D^F) + D^F * F^{\mathcal{G}}))\end{aligned} \tag{32}$$

While the closed form for L-hop neighbor is not feasible, we re-write $\#Nbrs(\mathcal{V},4)$ using its recursive nature,

$$\begin{aligned}\#Nbrs(\mathcal{V},4) =& O(D^{\mathcal{G}} * (D^{\mathcal{G}} * \#Nbrs(\mathcal{V},2)) + D^F * F^{\mathcal{G}} D^{\mathcal{G}} + (D^F)^2 F^{\mathcal{G}} \\ &+ D^F * F^{\mathcal{G}} * \#Nbrs(\mathcal{V},2) + D^F * F^{\mathcal{G}})\end{aligned} \tag{33}$$

where $\#Nbrs(\mathcal{V},2)$ contains $D^F * F^{\mathcal{G}}$. Thus, we see that $D^{\mathcal{G}}$ grows with the power of the number of hops L, and $D^F * F^{\mathcal{G}}$ multiplies after every other hop. Consequently, we approximate $Nbrs(\mathcal{V},L)$ as

$$\#Nbrs(\mathcal{V},L) \approx O((D^{\mathcal{G}})^L + (D^F)^{L/2} * (F^{\mathcal{G}})^{L/2}) \tag{34}$$

□.

B.2 Proof of corollary 1

We can see this via the personalized page-rank (PPR) equation for a target node v defined as

$$\pi(v) = (1-\alpha)\tilde{\mathcal{A}}\pi(v) + \alpha\mathbf{i}_v \tag{35}$$

where $\tilde{\mathcal{A}}$ is normalized with added self-loops, $\mathbf{i}_v$ is an indicator vector with indices except corresponding to node v are filled with 0 and $\alpha \in (0,1)$ is teleportation probability facilitating transportation to target node v in restart. Under conditions defined in PageRank-Nibble (Andersen et al., 2006), this equation equation can be expanded as,

$$\pi(v) = \alpha * \mathbf{i}_v(\mathrm{I} - (1-\alpha)\tilde{\mathcal{A}})^{-1} = \alpha * \sum_{r=0}^{i=\infty}(1-\alpha)^r\tilde{\mathcal{A}}^r\mathbf{i}_v \tag{36}$$

I is an identity matrix the same size as $\tilde{\mathcal{A}}$. As seen in the equation, the nearest nodes have a higher weightage of $(1-\alpha)$, which decays exponentially $(1-\alpha)^r$ with longer hops, where r is the shortest distance from the target node. The *feature-as-node* transformation used to construct $\mathcal{G}^{meta}$ introduces 2-hop paths for a pair of nodes (u,v) sharing at-least a single feature f as $v \to f \to u$ in $\mathcal{G}^{meta}$. Thus, the proposed transformation adds shorter paths between nodes that were originally farther in the $\mathcal{G}$, thereby improving their relative personalized page ranks. □.

B.3 Neutag is an Approximation of a Sparse Transformer Performer: Proof of theorem 2

We use a similar strategy outlined in (Cai et al., 2023), which showed that global nodes can approximate Performer. First, we rewrite the equation 17 as follows to simplify the analysis.

$$\mathbf{h}_i^{l+1} = \frac{\phi_1(\mathbf{h}_i^l)^T \sum_{j=1}^{j=N} \phi_2(\mathbf{h}_j^l) \otimes \phi_3(\mathbf{h}_j^l)}{\phi_1(\mathbf{h}_i^l)^T \sum_{o=1}^{o=N} \phi_2(\mathbf{h}_o^l)} \tag{37}$$

where we define $\phi_1(\mathbf{h}) = \phi(\mathbf{W}_Q\mathbf{h})$, $\phi_2(\mathbf{h}) = \phi(\mathbf{W}_K\mathbf{h})$, and $\phi_3(\mathbf{h}) = \mathbf{W}_V\mathbf{h}$. This allows us to use MLPs' universal approximation capability in the attention and aggregation equations. Intuitively, feature nodes can facilitate approximation of both global summations $\sum_{j=1}^{j=N} \phi_2(\mathbf{h}_j) \otimes \phi_3(\mathbf{h}_j)$ and $\sum_{o=1}^{o=N} \phi_2(\mathbf{h}_o)$ because each graph node is connected to at least 1 feature node.

To prove theorem 2, we assume that in 15, $\mathbf{H}_{\mathcal{V}:local}$ is ignored by $\textsc{update}_1^l$ as local connectivity of graph nodes is not required to approximate Performer attention. We further subdivide layer l of Neutag into $(l1, l2, \ldots)$ for the purpose of this analysis.

Now, at layer l, we are given $\mathbf{h}_v \forall v \in \mathcal{V}$, For feature nodes $f \in \mathcal{V}^f$, let the representation include a one-hot identity vector as $\mathbf{h}_f = [\ldots, \mathbb{I}_f]\ \forall$ where $\mathbb{I}_f$ is a one-hot indicator vector with all zeros except f^{th} index, which

is equal to 1. This indicator vector is preserved from layer $l = 0$ and facilitates computation of feature degree d_v^F for every graph node v.

Next, using equations 11 and 16 and by learning equal attention coefficients for all present feature nodes, each graph node $v \in \mathcal{V}$ approximates either of the two representations as follows.

$$\textbf{1)}\ [\phi_2(\mathbf{h}_v^l),\ (\phi_2(\mathbf{h}_v^l) \otimes \phi_3(\mathbf{h}_v^l))_{\text{flattened}},\ d_v^F] \quad \text{or} \quad \textbf{2)}\ [\phi_2(\mathbf{h}_v^l)/d_v^F,\ (\phi_2(\mathbf{h}_v^l) \otimes \phi_3(\mathbf{h}_v^l))_{\text{flattened}}/d_v^F]$$

where flattened signifies flattening of the matrix to a vector. This corresponds to sub-layer $l1$.

At sub-layer $l2$, each feature node $f \in \mathcal{V}^f$ using equation 12, learn attention coefficients $\frac{1}{d_v^F}$ for all $v \in \mathcal{N}_f^{\mathcal{G}}$ and computes vector

$$\Big[\sum_{v \in \mathcal{N}_f^{\mathcal{G}}} \phi_2(\mathbf{h}_v^l)/d_v^F, \quad \sum_{v \in \mathcal{N}_f^{\mathcal{G}}} (\phi_2(\mathbf{h}_v^l) \otimes \phi_3(\mathbf{h}_v^l))_{\text{flattened}}/d_v^F, \quad \mathbb{I}_f \Big].$$

The one-hot indicator vector $\mathbb{I}_f$ is required to ensure a distinct representation for each feature node and to allow for feature-degree statistics at graph nodes in consecutive layers. A similar representation can be learned in Case 2 using equal attention coefficients.

Finally at sub-layer $l3$, feature nodes can spread these partial statistics to each graph node using both positive and negative attention paths and consecutively graph nodes can aggregate partial statistics into global $[\sum_{v=1}^{v=N} \phi_2(\mathbf{h}_v^l), \sum_{v=1}^{v=N} (\phi_2(\mathbf{h}_v^l) \otimes \phi_3(\mathbf{h}_v^l))_{flattened}]$ using equations 11,14 and eq. 15 and approximate the required PERFORMER layer 37 using eq. 15 in this final aggregation step.

Alternatively, at sub-layer $l3$, all-pair feature-to-feature attention path facilitates each feature node $f \in \mathcal{V}^f$ to learn equal attention weight of $\frac{1}{F}$ and aggregate global sums $[\sum_{v=1}^{v=N} \phi_2(\mathbf{h}_v^l), \sum_{v=1}^{v=N} (\phi_2(\mathbf{h}_v^l) \otimes \phi_3(\mathbf{h}_v^l))_{flattened}, \mathbb{I}_f]$ using eq. 10 and 16. At sub-layer $l4$, each graph node $v \in \mathcal{V}$ retrieves these global sums using eq. 11 and compute the required performer attention layer 37 using eq. 15.

Either of these two approximation pathways is sufficient to approximate the PERFORMER layer. Consequently, the number of parameters required in each layer of NEUTAG to approximate a PERFORMER layer remains constant with respect to the number of nodes N. □.

B.4 Universal Approximation Analysis of Neutag

Dense transformers have been proven universal approximations of sequence-to-sequence permutation equivariant functions (Yun et al., 2020). The same work further proves that transformers are universal approximators of all sequence-to-sequence functions by including position encoding. Further SAN (Kreuzer et al., 2021a) proves that since a graph can be constructed as a sequence of edges or nodes, dense attention-based graph transformers are universal approximates of such sequences within a bound, inducing higher expressivity than 1-Weisfeiler Lehman (WL) isomorphism test. Since NEUTAG doesn't utilize all $\mathcal{O}(N^2)$ connections, analyzing its universal approximation capabilities is important. Formally,

Theorem 3. *Under the stated assumptions, for a given input graph $\mathcal{G}$, its transformed graph $\mathcal{G}^{meta}$, and node representation matrix $\mathbf{X} \in \mathbb{R}^{N \times d}$, there exists a NEUTAG attention layer that can approximate the following all-pair self-attention operation as a permutation-equivariant universal approximator, using $\mathcal{O}(N^d)$ parameters and $\mathcal{O}(1)$ layers:*

$$\mathbf{H} = \text{SOFTMAX}\left(\frac{(\mathbf{H}^l\mathbf{W}_Q)(\mathbf{H}^l\mathbf{W}_K)^T}{\sqrt{d}}\right)\mathbf{H}^l\mathbf{W}_V \tag{38}$$

This holds under the following assumptions: (i) each graph node $v \in \mathcal{V}$ is connected to at least one feature node $f \in \mathcal{V}^f$ in $\mathcal{G}^{meta}$, and (ii) the model has sufficient capacity $\mathcal{O}(N^d)$.

Proof: Similar to (Cai et al., 2023), we first relate NEUTAG to DEEPSETS (Zaheer et al., 2017), which is a universal approximator of sequence-to-sequence permutation equivariant functions. Formally, we define the following lemma.

Definition 2 (DeepSets (Zaheer et al., 2017)). *Each layer of DEEPSETS is defined as follows.*

$$\mathbf{H}^{l+1} = \sigma(\mathbf{H}^l\mathbf{W}_1 + \frac{1}{N}\mathbf{1}\mathbf{1}^T\mathbf{H}^l\mathbf{W}_2) \tag{39}$$

where σ is a non-linearity activation function, $\mathbf{H}^l$ is output of previous layer, $\mathbf{1} = [1, 1, \ldots]^T$ is N dimensional vector and $\mathbf{W}_1$, $\mathbf{W}_2$ are learnable weight matrices.

$\frac{1}{N}\mathbf{1}\mathbf{1}^T$ calculates the average of transformed inputs $\mathbf{H}^l\mathbf{W}_2$, producing a permutation-equivariant function. ,which is added to $\mathbf{H}^l\mathbf{W}_1$. This function can easily be verified as permutation-equivariant, since node reordering only permutes the output. Now, we formally write the following lemma of (Segol & Lipman, 2019).

Lemma B.1 ((Segol & Lipman, 2019))**.** *DeepSets with $\mathcal{O}(1)$ layers and $\mathcal{O}(N^d)$ parameters per layer is a universal approximator for permutation equivariant sequence to sequence functions.*

Thus, DeepSets can approximate the self-attention operation in eq. 38, which is a permutation equivalent function. Similar to the proof of theorem 2, both operations in DeepSets, **a)** calculating the average of node embeddings and **b)** adding the calculated average to the node representation and applying σ can be simulated by Neutag leveraging the fact that each graph node is connected to at least one feature node. And since DeepSets can approximate equation 38, the result follows. □.

Consequently, while the theorem shows that the proposed transformation is theoretically capable of approximating a dense self-attention layer, this does not imply that such an approximation is achievable with a realistic number of model parameters, especially for large-scale graphs.

Practical scope and limitations: The above result shows that Neutag can approximate a dense self-attention layer under the stated assumptions. Though this does not imply exact equivalence in practical settings, particularly, the construction in the proof requires $\mathcal{O}(N^d)$ parameters, which is impractical for real-world graphs. Therefore, this result primarily serves as theoretical grounding for the proposed attention mechanism.

C Extension of Neutag to real-valued attributed graphs

Given a real-valued attributed graph $\mathcal{G} = (\mathcal{V}, \mathcal{E}, \mathbf{X}^{real})$, we aim to convert it to $\mathcal{G} = (\mathcal{V}, \mathcal{E}, \mathbf{X}^{binary})$ where $\mathbf{X}^{real} \in \mathbb{R}^{N\times d}$ and $\mathbf{X}^{binary} \in \{0, 1\}^{N\times d'}$. To achieve this, we utilize the theory of knowledge distillation (Hinton et al., 2015). We first train a teacher model $\theta_{teacher}$, a 2-layer MLP with input $\mathbf{X}^{real}$, on the node classification task. Please note that graph topology is not used for this training. For the student model, we adopt the $k - sparse$ encoder (Makhzani & Frey, 2013).

$$\Gamma = \text{supp}_k(\mathbf{X}^{real}\mathbf{W}) \tag{40}$$

$$\mathbf{X}^{binary}_{\Gamma} = 1, \quad \mathbf{X}^{binary}_{\Gamma^{\complement}} = 0 \tag{41}$$

Here $\mathbf{W} \in \mathbb{R}^{d\times d'}$,$\text{supp}_k$ selects the k indices corresponding to k largest activation. Finally, we set those indices to 1 and the rest to 0 in $\mathbf{X}^{binary}$. Finally, we train the student network using the following knowledge-distillation loss.

$$\mathbf{L}^{teacher} = \text{SOFTMAX}(\text{MLP}_{\theta^{teacher}}(\mathbf{X}^{real})) \tag{42}$$

$$\mathbf{L}^{student} = \text{SOFTMAX}(\text{MLP}_{\theta^{student}}(\mathbf{X}^{student})) \tag{43}$$

$$\mathcal{L} = (1 - \lambda)\text{KL}(\mathbf{L}^{teacher}, \mathbf{L}^{student}) + \lambda\text{CE}(\mathbf{Y}, \mathbf{L}^{student}) \tag{44}$$

where $\mathbf{L}^{teacher}$ and $\mathbf{L}^{student}$ are class probabilities from teacher and student models respectively. KL is a KL-divergence loss, and CE is a cross-entropy loss for the classification task. $\mathbf{Y}$ is a ground truth vector. λ is a hyper-parameter to adjust the weightage between KL divergence loss and cross-entropy loss. We note that $\theta^{teacher}$ is fixed from the teacher model, and $\mathcal{L}$ is used to train the $\theta^{student}$ and $\mathbf{W}$ matrix from eq. 40.

We use $\lambda = 0.1$. The transformed $\mathbf{X}^{binary}$ vectors can achieve classification accuracy within $\sim 10 - 15\%$ margin compared to $\mathbf{X}^{real}$ vector on the classification task using a MLP without graph topology as input. Specifically, in OBGN-Arxiv, $\mathbf{X}^{real}$ achieves 53% accuracy while $\mathbf{X}^{binary}$ achieves 47%. In the case of OGBN-Arxiv(year), it is 33% vs 29%.

D Additional Experimental Details

D.1 Datasets

Cora (Sen et al., 2008) and CiteSeer(Yang et al., 2016) are co-citation graphs where nodes are papers, and their features are bag-of-words of text. The task is to predict the research category of the node. Actor (Pei et al., 2020) is a co-occurrence graph of actors on the same wiki page. Node attributes are bag-of-words from the actor's Wikipedia page, and their labels are actor categories. Chameleon (Rozemberczki et al., 2021) is a graph of hyperlinks between English wiki pages, attributes are nouns, and the label is the binned average monthly traffic on the page. Snap-patents (Lim et al., 2021) is a large-scale co-citation graph of U.S. utility patents where attributes are patent metadata and class label is the time at which the patent was granted, binned in 5 classes. OGBN-Arxiv (Hu et al., 2020) is also a co-citation network where features are 128-dimension embeddings of title and abstract, and the label is the research category. OGBN-Arxiv(Year) is the same graph, but the label is the year of publication, and it is a non-homophilic graph. $\mathbf{H}_{edge}$ (Zhu et al., 2020) in table 5 denotes the edge homophily of a graph.

Table 5: Dataset statistics

Dataset	# Nodes	# Edges	# Features	#Labels	$\mathbf{H}_{edge}$	Avg. features per node
Cora	2708	10556	1433	7	0.81	≈ 18
CiteSeer	3327	9104	3703	6	0.74	≈ 32
Actor	34493	495924	8415	5	0.22	≈ 5
Chameleon	7600	33544	931	5	0.23	≈ 13
OGBN-Arxiv	169343	1166243	128	40	0.81	128
OGBN-Arxiv(year)	169343	1166243	128	5	0.22	128
Snap-Patents	2923922	13975788	269	5	0.07	5

D.2 Hardware Details

We have performed experiments on an Intel Xeon 6248 processor with a Tesla V-100 GPU with 32GB GPU memory and Ubuntu 18.04. Train, validate, and test data split of 60%, 20%, and 20%, which are generated randomly for every run. We perform 5 runs of every experiment to report the mean and standard deviation. We use $4-6$ layer NEUTAG for small graphs and 2 layer for large graphs. We use Adam optimizer to train the model using a learning rate of 0.00001 and choose the best model based on validation loss. For all methods, including baselines and NEUTAG, we apply laplacian position encodings for small-scale datasets, and node2vec based position encoding in the snap-patent dataset, as laplacian position encoding calculation is computationally infeasible at million-scale datasets, as proposed in GOAT, for large-scale datasets. These are further used in NAGPHORMER and LARGEGT. For all experiments, we use the best hyper-parameters outlined in the respective baseline code-bases wherever available for each dataset. Otherwise, standard tuning is done for key hyper-parameters including the number of layers, embedding size, and number of virtual nodes where applicable. We have updated this in Appendix section D.2 of revised manuscript. We select a number of negative features per node using hyperparameter tuning over the range 1-10.

E Additional Results

E.1 Ablation Study

We design 5 variants of NEUTAG, **1)**NEUTAG (COMPLETE) which is the entire architecture **2)** NEUTAG (LOCAL NBRS.), which only consists of attention with local neighbors **3)**NEUTAG$^+$ consists of attentions with local neighbors, feature nodes and feature to feature attention path except attention with negative features **4)**NEUTAG-F2F consists of all attention paths except feature to feature attention and **5)**NEUTAG$^+$-F2F consists of local neighbor attention and feature node attention. Table 6 demonstrates the effectiveness of all the variants. Specifically, we observe that computing node representation by only attending to local neighbors NEUTAG (LOCAL NBRS) results in sub-optimal performance across all datasets. The performance drop is much more significant in non-homophilic graphs Actor and Chameleon. This signifies the importance of various attention paths involving feature nodes in learning both homophilic and heterophilic biases in NEUTAG.

Table 6: Ablation of NEUTAG on node classification task

Neutag Variants	Cora	CiteSeer	Actor	Chameleon
NEUTAG (COMPLETE)	87.26 ± 2.14	76.00 ± 0.99	$\mathbf{36.25 \pm 2.43}$	$\mathbf{65.26 \pm 2.43}$
NEUTAG (LOCAL NBRS.)	81.01 ± 3.67	75.49 ± 1.10	25.52 ± 0.87	30.70 ± 1.49
NEUTAG$^+$	87.19 ± 0.96	$\mathbf{77.68 \pm 1.9}$	34.93 ± 0.83	64.07 ± 2.73
NEUTAG $-$F2F	87.12 ± 1.46	75.70 ± 0.3	34.26 ± 1.85	63.02 ± 3.79
NEUTAG$^+-$F2F	$\mathbf{87.67 \pm 1.10}$	74.65 ± 0.95	34.93 ± 0.46	64.12 ± 1.95

Table 6 also indicates that attention with local neighbors and feature nodes (NEUTAG$^+-$F2F) is competitive across all datasets. In contrast, additional attention with negative feature nodes and feature-to-feature attention NEUTAG (COMPLETE) provides a performance boost in heterophilic graph Actors and Chameleon.

Moreover, we also perform ablation of NEUTAG with respect to the number of negative feature nodes sampled per graph node to analyze the sensitivity of NEUTAG with respect to the number of negative feature samples. Figure 4 shows that performance improves with increasing number of negatives, but it saturates quickly at around 5.

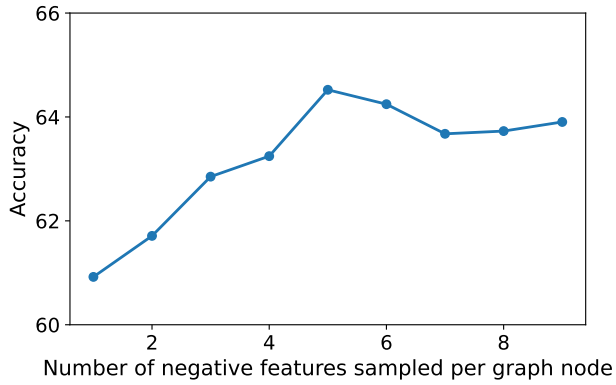

Figure 4: Impact of number of negative feature sampling on model performance on Chameleon dataset

E.2 Additional Challenging Heterophilic datasets

We further benchmark NEUTAG on challenging heterophilic datasets, with graph statistics and results summarized in Table 7. As shown, NEUTAG consistently outperforms scalable graph transformers.

Table 7: Comparison of NEUTAG with scalable GT on additional challenging heterophilic graphs (Luan et al., 2024a)

Dataset	**# Nodes**	**# Edges**	$\mathbf{H}_{edge}$	**# Features**	**Avg. feat./ node**	NAGPHORMER	GOAT	LARGEGT	NEUTAG
Facebook	4039	88234	0.5816	1283	≈ 8	59.91 ± 1.11	Error	Error	$\mathbf{63.09 \pm 1.29}$
Cornell	183	295	0.2983	1703	≈ 94	58.90 ± 5.23	67.02 ± 8.41	53.51 ± 11.89	$\mathbf{77.834 \pm 7.33}$
Squirrel	5201	217073	0.2234	2089	≈ 18	38.05 ± 2.00	33.56 ± 0.74	36.5 ± 2.69	$\mathbf{50.36 \pm 2.12}$
Wisconsin	251	499	0.1703	1703	≈ 96	58.42 ± 4.01	74.11 ± 7.76	69.01 ± 7.48	$\mathbf{78.034 \pm 4.19}$
Texas	183	309	0.0615	1703	≈ 83	60.61 ± 7.15	68.64 ± 4.09	68.10 ± 10.99	$\mathbf{82.69 \pm 4.04}$

E.3 Impact of missing features on Neutag

We conduct two studies to examine how missing features affect NEUTAG. The first study looks at missing features only during the graph transformation stage. Here, the original input features are intact, but node–feature edges are randomly removed to simulate different levels of feature sparsity.

Table 8: Comparison of NEUTAG with scalable GT on additional NAGPHORMER datasets

Dataset	# Nodes	# Edges	H_{edge}	# Features	Avg. feat./ node	NAGPHORMER	GOAT	LARGEGT	NEUTAG
Pokec	1.6M	30.62M	0.4449	65	≈ 20	71.55 ± 2.40	Error	70.70 ± 0.21	$\mathbf{71.97 \pm 0.22}$
Photo	7850	238163	0.8272	745	≈ 259	94.32 ± 0.52	$\mathbf{95.58 \pm 0.45}$	93.76 ± 0.89	94.98 ± 0.39
Computer	13752	491722	0.7772	767	≈ 267	88.90 ± 0.70	$\mathbf{91.55 \pm 0.59}$	87.39 ± 1.10	90.50 ± 0.32
CoraFull	19793	126842	0.5670	8701	≈ 57	70.03 ± 0.91	69.21 ± 0.64	63.25 ± 0.65	$\mathbf{72.62 \pm 0.44}$

We test this on the Chameleon dataset. Dropping feature connections reduces the number of feature–node edges, which lowers the homophily of the transformed graph $\mathcal{G}^{meta}$. This weakens the structural connectivity of the transformed graph and, as expected, leads to a drop in classification accuracy, as shown in the table below.

Feature Drop Rate in $\mathcal{G}^{meta}$	$\text{Homophily}^{\mathcal{G}}_{ppr}$	$\text{Homophily}^{\mathcal{G}^{meta}}_{ppr}$	**Accuracy**
0%	0.2349	0.2807	65.26 ± 2.74
50%	0.2349	0.2615	60.51 ± 2.15
90%	0.2349	0.2398	58.45 ± 2.26

Table 9: Effect of feature drop rate during graph transformation on homophily and accuracy.

In another study, for completeness, we now randomly drop features with varying probability (p) from the input node feature matrix itself and benchmark it against the baseline methods in table 10. We observe that NEUTAG maintains relatively strong performance even under severe feature dropout, suggesting robustness to missing input features. This is an encouraging result. That said, we believe a comprehensive study on robustness under various real-world noise and corruption settings is a significant task that warrants a separate investigation.

E.4 Training Time and Memory Analysis

To empirically understand the scalability of NEUTAG, we measure the training time and GPU memory of NEUTAG vs other scalable GT. The following table 11 reports the training time across large-scale datasets Snap-patents, Pokec, and Arxiv.

Among baselines, NEUTAG emerges as the second-fastest, and NAGPHORMER is the fastest to compute attention over layers, while other methods, including NEUTAG, compute attention over nodes.

Moreover, Table 12 shows the parameter sizes of NEUTAG and the baselines on the large-scale snapshot-patent dataset. All models are lightweight in terms of parameter size.

E.5 Comparison of Neutag with Dense-Attention

To empirically evaluate how well NEUTAG approximates dense attention, we compare it with GRAPHGPS without the GNN component (GRAPHGPS-GNN). Removing the GNN module results in a model that relies solely on transformer-based global attention over nodes, effectively working as a dense-attention graph transformer. Table 1 reports the performance comparison. For clarity, we reproduce the relevant results here in table 13. As shown, NEUTAG achieves comparable or better results, empirically supporting the theoretical analysis presented in theorem 2.

E.6 Analysis of Structural vs. Feature-based Attention Paths

To better understand how NEUTAG combines structural information from local neighborhood 9 and global information from feature nodes 11 based on the underlying graph characteristics for node classification, we analyze the relative contribution of each component to the final node representation 15. For this analysis, we consider the linear projection component $\text{MLP}^{L}_{1}(\mathbf{H}^{l}_{\mathcal{V}:local} \mid \mathbf{H}^{l}_{\mathcal{V}:+})$ in eq. 15, rewriting it for a graph node $v \in CV$ as follows.

Method	$p = 0$	$p = 0.5$	$p = 0.9$
GraphSage	48.95 ± 3.16	44.42 ± 2.04	37.50 ± 2.81
Gat	44.74 ± 3.29	38.33 ± 3.73	34.20 ± 1.46
Gin	32.68 ± 3.68	31.22 ± 1.02	30.26 ± 3.54
MixHop	47.68 ± 2.89	38.13 ± 5.12	31.14 ± 3.54
Linkx	48.20 ± 3.31	42.19 ± 1.58	35.26 ± 3.04
GraphGPS	42.88 ± 1.88	36.14 ± 2.73	32.96 ± 3.77
Exphormer	45.17 ± 2.56	42.45 ± 1.60	35.43 ± 1.04
NagPhormer	59.97 ± 1.72	56.72 ± 1.90	58.56 ± 1.31
Goat	53.28 ± 2.48	43.85 ± 1.93	34.56 ± 2.50
LargeGT	57.19 ± 1.89	55.24 ± 2.45	52.58 ± 1.70
Neutag	$\mathbf{65.26 \pm 2.43}$	$\mathbf{60.40 \pm 0.99}$	$\mathbf{58.75 \pm 2.06}$

Table 10: Performance of different methods under varying feature drop rates (p).

Dataset	N(Millions)	M (Millions)	NagPhormer	Goat	LargeGT	Neutag
Snap-patents	2.92	13.97	1.1	> 24	14	6
Pokec	1.62	30.62	0.56	ERROR	5.5	4.2
Arxiv	0.16	1.16	0.086	7.7	0.6	1.5

Table 11: Training time comparison of Neutag with baselines (Hrs.)

$$\mathbf{h}_v^{final} = \mathbf{W} \cdot [\mathbf{h}_v^{struct} \mid \mathbf{h}_v^{global}] \tag{45}$$

where $\mathbf{h}^{struct}$ denotes the representation aggregated from graph neighbors $\mathcal{V} : local$, and $\mathbf{h}^{global}$ denotes the representation aggregated from feature nodes $\mathcal{V} : +$. Now weight matrix $\mathbf{W}$ in eq. 45 can be decomposed as follows.

$$\mathbf{W} = [\mathbf{W}_{struct}\ \mathbf{W}_{global}] \tag{46}$$

Thus, the eq. 45 can be expressed as:

$$\mathbf{h}_v^{final} = \mathbf{W}_{struct}\mathbf{h}_v^{struct} + \mathbf{W}_{global}\mathbf{h}_v^{global} \tag{47}$$

Now, to quantify the contribution of local neighbors(structural) and global information, we measure the magnitude of the corresponding projected representation. For a graph node $v \in \mathcal{V}$, let us define,

$$C_v^{struct} = \|\mathbf{W}_{struct}\mathbf{h}_v^{struct}\|_2, \quad C_v^{global} = \|\mathbf{W}_{global}\mathbf{h}_v^{global}\|_2 \tag{48}$$

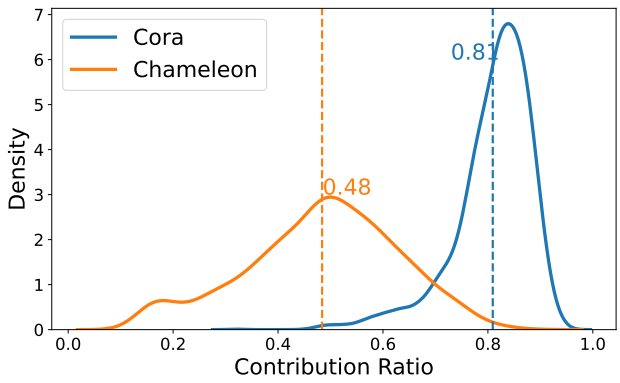

Figure 5: Local neighborhood vs. feature-based attention contribution

NeuTAG	LargeGT	Goat	NagPhormer
742361 (3 MB)	403462(1.6 MB)	442125(1.77 MB)	176519(706 kb)

Table 12: Parameter sizes of NeuTAG and baselines on Snap-patents dataset

Method	Cora	CiteSeer	Actor	Chameleon	OGBN-Arxiv	OGBN-Arxiv(Year)	Snap-patents
GraphGPS-Gnn	72.47 ± 1.87	71.59 ± 2.43	37.10 ± 1.11	47.36 ± 2.22	OOM	OOM	OOM
NeuTAG	$\mathbf{87.67 \pm 1.10}$	$\mathbf{77.68 \pm 1.90}$	36.21 ± 1.2	$\mathbf{65.26 \pm 2.43}$	70.63 ± 0.29	$\mathbf{53.96 \pm 0.38}$	63.00 ± 0.22

Table 13: Comparison of NeuTAG with respect to dense-attention

Consequently, we define the relative contribution of the structural component as follows for $v \in \mathcal{V}$:

$$R_v^{struct} = \frac{C_v^{struct}}{C_v^{struct} + C_v^{global}} \tag{49}$$

We analyze the distribution of R_v^{struct} across all nodes $\mathcal{V}$ in $\mathcal{G}$. We visualize this distribution for both homophilic graph Cora and heterophilic graph Chameleon in figure 5. Figure 5 clearly shows that NeuTAG primarily relies on local neighborhood with a concentrated distribution with mean of 0.81.

In contrast, on heterophilic Chameleon, the contribution distribution is highly balanced with mean ≈ 0.53 and shows high variance. This suggests that the model is able to leverage feature-based connections at the node level, rather than follow a fixed structural bias and use feature-based connections as needed. These observations demonstrate that NeuTAG can dynamically adapt to both homophilic and heterophilic graphs by utilizing and balancing both local neighborhood information and feature-based information.

E.7 Sensitivity to feature binarization for real-valued attributed graphs

We analyze the sensitivity of NeuTAG to the encoding dimension d' used in the k-sparse encoder for binarizing real-valued features (Appendix C).

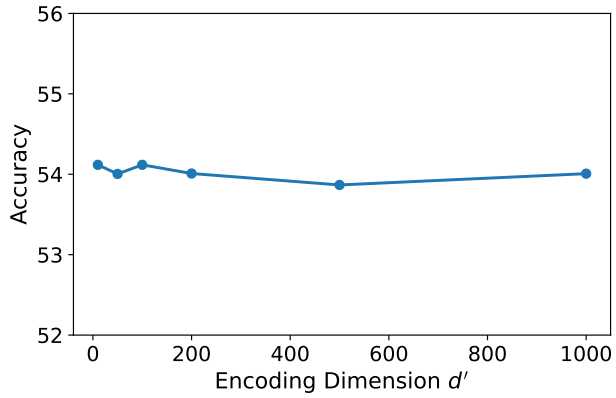

Figure 6: Sensitivity analysis of NeuTAG wrt. hyper-parameter d' used in k-sparse encoder for binarization of real-valued attributed features.

Figure 6 shows the performance across a wide range of $d' \in \{10, 50, 100, 200, 500, 1000\}$ with fixed $k = 10$. We observe that the downstream accuracy remains largely stable, with negligible variation across different values of d'. This indicates that the proposed binarization scheme is robust to the choice of encoding dimension and does not require careful tuning.

Similarly, we further investigate the sensitivity of NEUTAG to the sparsity hyperparameter k , which determines the top-k largest activations to be annotated as 1 and the rest as 0 during binarization. Figure 7 shows the performance of NEUTAG across a range of k. The performance improves as k increases from a very small value, showing that information loss in under-sparse representations, and it saturates with moderate values of k, suggesting NEUTAG is not highly sensitive once sufficient k is achieved.

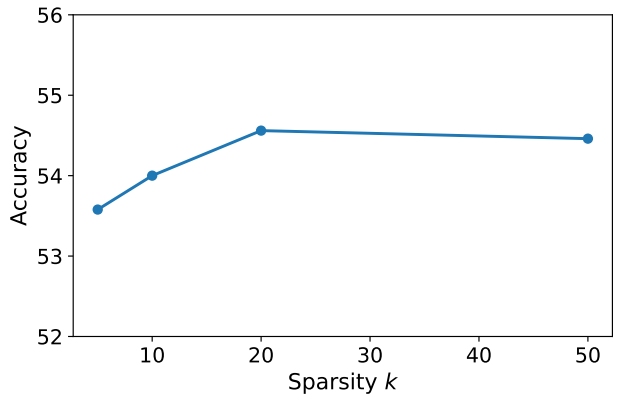

Figure 7: Sensitivity analysis of NEUTAG wrt. sparsity hyper-parameter k in k-sparse encoder for binarization of real-valued attributed features.